



The first rainfall erosivity database in Mexico: facing challenges of leveraging legacy climate data

Viviana Marcela Varón-Ramírez^{1,2}, Douglas A. Gómez-Latorre², Carlos Eduardo Arroyo-Cruz¹, Alberto Gómez-Tagle³, Blanca Lucía Prado Pano⁴, Ronald R. Gutierrez Llantoy⁵, Deyanira Lobo-Luján⁶, and Mario Guevara¹

¹Instituto de Geociencias - Universidad Nacional Autónoma de México - UNAM. Campus Juriquilla, Qro. Mexico.

²Corporación Colombiana de Investigación Agropecuaria - AGROSAVIA, Centro de Investigación Tibaitatá, Mosquera-Cundinamarca, Colombia

³Instituto de Investigaciones sobre los Recursos Naturales - INIRENA, Universidad Michoacana de San Nicolás de Hidalgo. Morelia, Mexico

⁴Instituto de Geología - Universidad Nacional Autónoma de México - UNAM. Mexico City. Mexico.

⁵Departamento de Ingeniería (GERDIS, GEOSD), Pontificia Universidad Católica del Perú. Lima, Peru

⁶Instituto de Edafología - Universidad Central de Venezuela. Maracay, Aragua. Venezuela

Correspondence: Viviana Marcela Varón-Ramírez (viviana.varon@geociencias.unam.mx) and Mario Guevara (mguevara@geociencias.unam.mx)

Abstract. Soil Water Erosion (SWE) is the dominant soil degradation driver on a global scale. For quantifying SWE, erosivity is an index that reflects the potential (i.e., the energy) of rainfall to cause SWE. To enhance the assessment of the SWE process at the national scale—, the objectives of this research are a) to develop the first Mexican rainfall time series database for three climate normals CNs (1968-1997, 1978-2007, and 1988-2017) leveraging legacy climate data, and b) to estimate rainfall erosivity across continental Mexico by using daily rainfall time series. The workflow has three methodological moments: 1) development of the rainfall time series database, 2) estimation of rainfall erosivity, and 3) rainfall erosivity verification. First, we compiled and harmonized over 5000 useful rainfall time series (RTS) well distributed across the Mexican territory. We performed a quality assurance, homogeneity analysis (using the normal homogeneity test), and data gap-filling (using the proportion method). Then, we use a potential power law equation to estimate rainfall erosivity at daily resolution. Finally, we compared and verified our results with three external datasets (global, national, and local scales). The principal research product is a new database with 1370, 1678, and 1676 RTS for each CN and its corresponding rainfall erosivity. The mean values for rainfall erosivity for the three CNs were 3600, 3296, and 3461 MJ mm ha⁻¹ h⁻¹ yr⁻¹, respectively. The statistical distribution of the erosivity values was right-skewed for the three CNs, with high erosivity values reaching >8000 MJ mm ha⁻¹ h⁻¹ yr⁻¹ in all the three CNs. About the verification of erosivity values, we found that Tropical rain-forests, temperate Sierras, and the Great Plains are the ecoregions with more significant differences concerning the global database, a generalized underestimation of erosivity values concerning the national dataset, and an adjustment coefficient of 1.85 for a local condition in Michoacan state. This new database provides tools for daily climatological analysis across Mexican territory and through a multiyear period (1968 to 2017). Erosivity results trigger the study of SWE at the national scale by identifying areas with higher susceptibility to soil loss due to rainfall action and providing a more spatially dense erosivity database that



20 follows the pattern of erosivity databases from higher time resolution. Following the FAIR principles (Findability, Availability, Interoperability, and Reproducibility) for scientific data, this database is available from a scholarly accepted repository (<https://doi.org/10.6073/pasta/7479676e406aeb40127da7b096b28eb2>) for public consultation.

Keywords: legacy climate data, gap filling of climate series, daily rainfall erosivity, climatol package

1 Introduction

25 Soil Water Erosion (SWE) refers to the soil displacement from its original location due to water action, such as rainfall, overland flow, and irrigation (Nearing, 2013). SWE represents the dominant soil degradation issue at the global scale because it affects nearly 33% of the World's surface (Pennock, 2019). The impact of SWE is not just on-site but also has off-site effects on distant locations. On-site, soil loses its natural fertility and capacity to store water, nutrients, and organic carbon (Hatfield et al., 2017), affecting food security. Off-site, the eroded soil triggers environmental issues such as water pollution,
30 dam siltation, eutrophication of water bodies, contamination of coastal and marine ecosystems, and overall environmental damage (Feng et al., 2023).

When other erosion factors (e.g. erodibility, soil coverage and management, and topography) are constant, regions with frequent rainfall experience more soil loss than areas with limited rainfall (Ke and Zhang, 2021). Rainfall erosivity is the potential of rainfall to cause SWE (Nearing et al., 2017). Furthermore, rainfall erosivity is the first-factor influencing SWE and
35 is crucial for soil and water conservation planning. As extreme rainfall events are expected to increase in tropical zones due to climate change, SWE will likely increase as well (Borrelli et al., 2020). For example, in Mexico, the temporal distribution of rainfall has become more extreme, with more extended periods of drought and increasingly extreme rainfall events (Porrúa et al., 2020). Thus, understanding rainfall erosivity patterns across Mexico is essential for enhancing soil sustainability and informed decision-making in soil conservation

40 Rainfall erosivity—often represented as the R factor—quantifies the potential of rainfall to cause SWE (Nearing et al., 2017). The R factor captures the combined effect of raindrop impact and water flow. This R factor, when calculated by rainfall event as the product of total storm energy (E) and the maximum 30-minute intensity (I_{30}) is notated as $R(EI_{30})$ factor. However, I_{30} necessitates high temporal resolution rainfall data, often at a minute temporal resolution, which can be challenging to obtain, especially at a national scale of Mexico. However, when coarser time intervals are used instead of minute
45 temporal resolution, the relationship between E and I_{30} remains consistent, but a more larger calibration coefficient is needed (Tu et al., 2023). For this reason, the finer the time interval of the rainfall time series (RTS) used to calculate the R factor, the closer the estimations are to the $R(EI_{30})$ values as originally defined in Musgrave (1947).

In Mexico, the finest temporal resolution of legacy climate data to estimate rainfall erosivity is daily. As in many countries around the world, there are some issues in the available Mexican rainfall time series, such as missing values, short measurement
50 periods, and series inhomogeneity (breaks due to station relocation and measurement mistakes), which further compound the challenge of using climate data (McKinnon, 2022). In that way, erosion studies in Mexico have calculated the R factor from coarse-resolution RTS (monthly or annual) for some specific regions (Benites et al., 2020; González et al., 2016). However,



a national estimation of the R factor does not exist (Varón-Ramírez and Guevara, 2024). Thus, climatology studies, such as erosivity, need a complete and reliable rainfall time series database (Yozgatligil et al., 2013). Therefore, a whole scheme of
55 quality assurance, gap-filling, and homogenization process of the rainfall time series is needed (WMO, 2023). Consequently, with a reliable rainfall database, it is possible to represent the actual rainfall characteristics in a particular region and allow soil erosion monitoring at the local and national scales in Mexico.

Developing a rainfall time series and, consequently, a rainfall erosivity database is challenging in both spatial and temporal terms. The large diversity of topographic conditions (i.e., two principal mountain ranges and a large latitudinal extent) and
60 proximity with large water bodies from the Pacific Ocean and the Gulf of Mexico makes Mexico a contrasting scenario of rainfall patterns (Carrera et al., 2024) and its hydrological-related processes (e.g., rainfall erosivity). Accurate benchmarks for understanding typical climate conditions and characterizing climate trends require a rainfall database long enough to represent its corresponding climate normal (CN), i.e., a statistical product computed over 30 years of rainfall time series (World Meteorological Organization, 2017). The CNs are widely used to compare recent observations, create anomaly-based datasets,
65 and provide context for future climate projections. Considering local patterns across different CNs, these characteristics will contribute to an unprecedented rainfall time series dataset to estimate rainfall erosivity in Mexico.

The lack of reliable and complete daily climate databases has not allowed the study of the impact of precipitation on the SWE process at a national scale in Mexico. Hence, the main objectives of this research are 1) to develop the first Mexican rainfall-series database for three climate normals (1968-1997, 1978-2007, and 1988-2017), leveraging on the availability of legacy
70 climate data, 2) to estimate rainfall erosivity across continental Mexico by using daily rainfall time series. The next section describes the three methodological moments of this research: rainfall time series database development, rainfall erosivity estimation, and rainfall erosivity verification. Then, the results are presented accordingly. We present discussion section with a critical analysis of results against recent scientific literature. We finally present our conclusions section; and the availability of all the codes and resulting databases of this research. The new knowledge allows a better understanding and prediction of
75 rainfall distribution and its associated processes in different regions of Mexico.

2 Methodology

The study area corresponds to the conterminous Mexico (1,948,170 km²). The country is located between latitudes 14°W and 32°N and longitudes 86°W and 118°W. Because of its geographical location, the region exhibits complex topographic and climate features (de Anda Sánchez, 2020). Mexico has been clustered by seven first level ecoregions—which represent
80 geographical units with characteristic flora, fauna, and ecosystems (Commission for Environmental Cooperation, 1997)—, namely: Mediterranean California, North American Deserts, Semi-arid Elevations, Great Plains, Tropical Rain Forest, Tropical Dry Forest, and Temperate Sierras. Each ecoregion occupies 1.3, 28.6, 11.8, 5.5, 14.2, 16.4, and 22.3 % of the total country area, respectively (Figure 1).

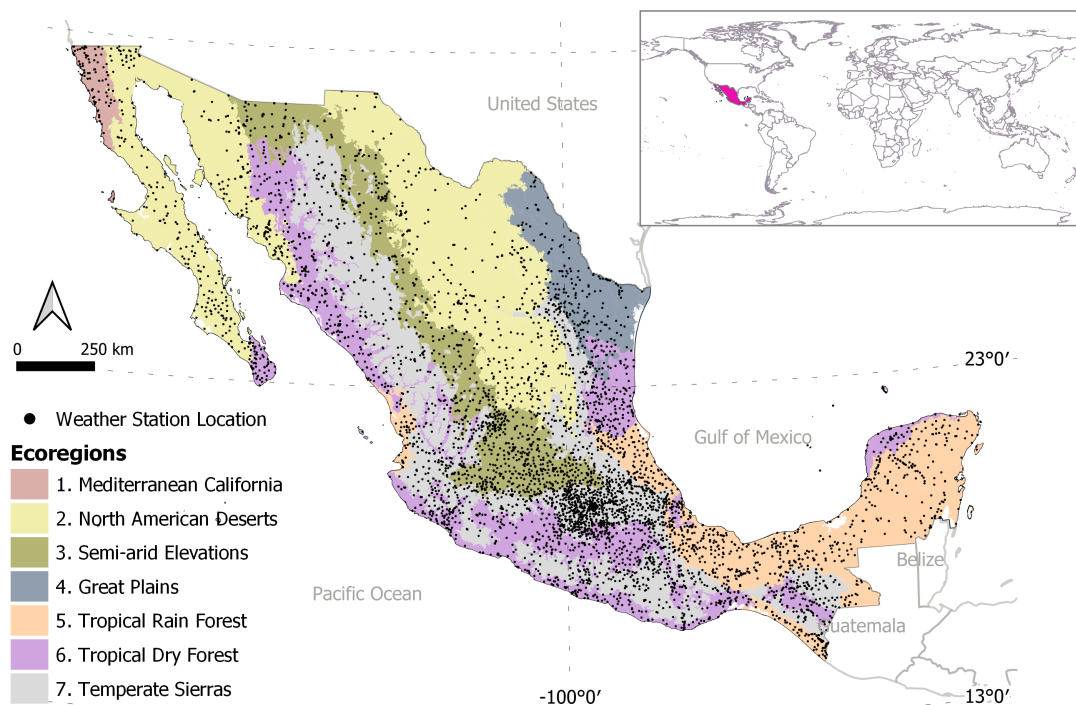


Figure 1. Ecoregions defined by the Commission for Environmental Cooperation (1997) and locations of the weather station available from the National Meteorological Service (SMN)

This research followed a workflow of three methodological stages (Figure 2). First, we developed a rainfall time series database with a daily resolution. Second, we estimated the rainfall erosivity by using daily rainfall time series. Third, we verified the rainfall erosivity estimations.

2.1 Rainfall time series (RTS) database development

The RTS database was developed through four steps: first, compilation, selection, and quality assurance of RTS. Second, the clustering of the RTS following its geographical and data attributes. Third, homogenization and data gap-filling of monthly and daily RTS. Fourth, quality control of the data gap-filling process.

2.1.1 Compilation, selection, quality assurance of RTS

In Mexico, the climate time series database results from the continuous effort of measuring, compiling, transcription, and analyzing data reported by weather stations distributed throughout the entire Mexican territory. This effort is led by the National Meteorological Service, which makes available to the public the raw data collected since 1900.

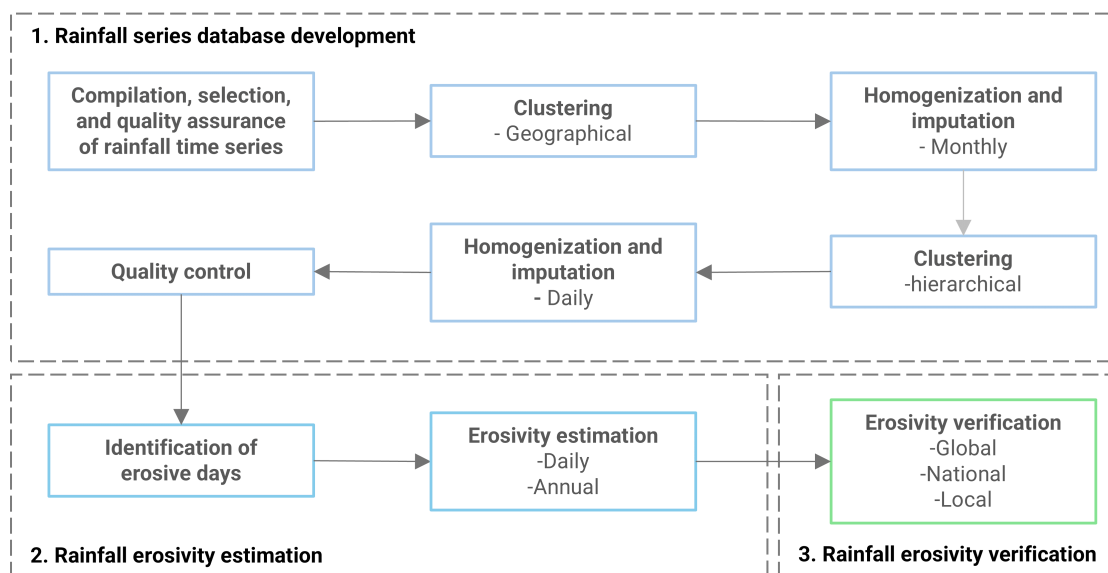


Figure 2. Workflow summarizing the three key methodological stages: (1) Development of the rainfall series database, (2) Estimation of rainfall erosivity, and (3) Verification of the calculated rainfall erosivity.

95 The data can be downloaded from the official National Meteorological Service site [<https://smn.conagua.gob.mx/es/>]. In the case of this project, 5454 files in plain-text format were downloaded, corresponding to the daily database of the entire network of weather stations (Fig. 1) available up to June 2022. Each file contains a header in which the weather station identification is reported and a series of data on its geographical location. Additionally, the files have daily data for rainfall, evaporation, and maximum and minimum temperature.

100 All data processing, including file downloading, was implemented in R (R Core Team, 2022). The download process was automated using the `download.file` function implemented in the `utils` package. A preparation pre-process facilitates the handling of data by separating the header's information and the daily data. The header data were extracted and converted to shapefile (`sic`) (`.shp`) format for spatial management. Subsequently, the file is converted in to a comma-delimited values format (`*.cvs`).

105 Finally, there were 5410 RTS at a daily temporal resolution with a unique format, and we considered those potentially useful RTS for our study. Consequently, there were two principal products in this step. First, a `*.csv` file with the information of the weather station, where each column corresponds to each of the data provided in the header (e.g., station ID, name, state, municipality, current situation, institution in charge, longitude, latitude, altitude, and report date), and each row corresponds to a weather station. Second, a set with 5410 `*.csv` files with the climate series of each weather station with four columns: date,
110 rainfall (mm), temperature ($^{\circ}\text{C}$), and relative humidity (%).



To select the useful RTS, we identified the standard period of registers for each RTS between 1961 and 2018. On the other hand, for erosivity estimations, it is recommended to use a historical RTS of ≥ 20 years (Vantas et al., 2019; Renard and Freimund, 1994). Therefore, this article looked over the RTS in three climate normals: CN1 (1968 to 1997), CN2 (1978 to 2007), and CN3 (1988 to 2017). Subsequently, we selected those RTS with less than 20% of missing values (WMO, 2023) for each climate normal.

Calculating the monthly cumulative rainfall, we identified that long sequences of zeros and NAs were common. For quality assurance, we identified those years with no rainfall and replaced zero values with NAs. Those RTS with less than 20% missing values after the replacement were included in the resulting rainfall dataset. However, we used those RTS as a reference in the data gap-filling step.

120 2.1.2 Clustering of rainfall time series (RTS)

Clustering analysis is highly recommended when gap-filling a large set of RTS (Guijarro, 2014). Clustering similar RTS allows you to use information from related series to fill in gaps. Rainfall patterns often exhibit spatial and temporal correlations, so data gap-filling from a group of similar series can result in more accurate estimates (Fransiska et al., 2024). In this workflow, we performed the data gap-filling by clustering the RTS according to 1) the geographical space, and the environmental characteristics of Mexico and 2) the data dissimilarity among diverse environments (Figure 2). The first clustering was performed using the ecological regions of North America (Commission for Environmental Cooperation, 1997; INEGI-CONABIO-INE, 2008). The second separation was performed after the data gap-filling and homogenization of monthly series by ecoregion. A hierarchical cluster analysis groups the data series with similar seasonality and rainfall volume patterns (Gómez-Latorre et al., 2022). The number of clusters (k) ranged from 2 to \sqrt{n} , where n is the total number of stations in the dataset (Rohlf, 1974). The better k values for each ecoregion were found using the Hartigan cluster validation index (Hartigan, 1975). This index was identified by Todeschini et al. (2024) to perform better when evaluating 68 cluster validation indexes (CVI's) over 21 different datasets. However, we did not perform a clustering analysis for Mediterranean California and Great Plains ecoregions due to the small size of the ecoregion and, therefore, the amount of the RTS available for those ecoregions.

2.1.3 Homogenization and data gap-filling of RTS

135 We followed three steps to get a complete RTS for each CN: quality assurance, homogeneity analysis, and data gap-filling (WMO, 2020). In this step, quality assurance involved verifying the physical and statistical consistency of the series, discarding outliers whose standardized anomaly was outside a predefined threshold and was unrelated to any climate variability events. Outliers are removed and replaced as NA values to be completed in the data gap-filling processes.

140 Homogeneity analysis involves removing the biases caused by some artificial breaks in the RTS (Yan et al., 2014). These breaks result from common issues such as reading or instrumental mistakes, instrumental changes, or special situations at the weather station location Guijarro (2014). We used the standard normal homogeneity test (Alexandersson, 1986) to analyze homogeneity.



To fill in missing data, we used the proportions method. This method estimates the missing information based on neighboring stations, considering the distance between each station (Paulhus and Kohler, 1952). The procedure used the three precipitation series with the highest correlation coefficient to the series that will be filled, with the condition of having been previously normalized. Then, we estimated $N_1 = \frac{A_1}{3} \left(\frac{N_a}{A_a} + \frac{N_b}{A_b} + \frac{N_c}{A_c} \right)$; where N_a , N_b and N_c are the precipitation data for each of the stations with the highest correlation, while A_a , A_b and A_c are their corresponding normal average. All of the data gap-filling and homogenization process was made with `homogen` function of `climatology` package (Guijarro, 2024).

Appendix A1 presents a summary of the homogenization parameters used for each step. Table A1 shows the parameters used to homogenize the monthly series, while Table A2 shows the parameters used to homogenize daily series by ecoregions 2, 3, 5, 6, and 7 and their corresponding subgroups.

2.1.4 Quality control of the data gap-filling processes

A quality validation was performed using the McCuen test (McCuen, 2016) to ensure consistency during the data gap-filling process of the rainfall time series. McCuen test compares the differences between the aggregated rainfall of the original multi-annual monthly means and the final series. The generated RTS with a difference greater than 10% related to its original were discarded.

2.2 Rainfall erosivity estimation

The days with erosive rainfall were identified as those with cumulative precipitation greater than 12.5 mm as an extension of the suggestion by Wischmeier and Smith (1978); Shin et al. (2019); Efthimiou (2018). After, we calculated daily erosivity R_d using the power law model proposed by Richardson et al. (1983); Alves et al. (2022); Beguería et al. (2018) with the sinusoidal relationship to describe the annual cycle of the coefficient of the power law function to represent seasonal differences in rainfall characteristics (Yu and Rosewell, 1996). Equation 1 presents the mathematical definition of R_d .

$$R_d = \alpha [1 + \eta \cos(2\pi f j - \omega)] P_d^\beta \quad (1)$$

where R_d is the daily erosivity, P_d is the daily precipitation; α , η , and β are adjusted coefficients; f is the monthly frequency (1/12); ω is $7\pi/6$; and j is the j -month of the year. The adjusted coefficients were adopted as in Xie et al. (2016), which utilized sixteen RTS at a one-minute temporal resolution to find the regression coefficients for the potential law equation.

The annual erosivity R_y ($\text{MJ mm ha}^{-1} \text{ h}^{-1} \text{ yr}^{-1}$) was calculated as the sum of the daily erosivity values in a year time ($R_y = \sum_{i=1}^{ed} R_{d_i}$). The rainfall erosivity R corresponds to the mean of the annual erosivity values for a multi-year period ($R = \sum_{j=1}^{30} R_{y_j}$). It is worth clarifying that, as we calculated the annual rainfall based on daily rainfall erosivity, estimated with the equation of Xie et al. (2016), we denoted those values as R (Xie et al. 2016). Finally, we obtained three datasets with rainfall erosivity values for the three climate normals: Mexico-CN1 (1968-1997), Mexico-CN2 (1978-2007), and Mexico-CN3 (1988-2017).



2.3 Rainfall erosivity verification

The rainfall erosivity values in the resulting datasets (Mexico-CN1, Mexico-CN2, and Mexico-CN3) were verified using three
175 databases at the global, national, and local scales. On a global scale, we used the GloREDA database (Panagos et al., 2023); at
the national scale, we used the database obtained by Torres (1991); and at the local scale, we calculated rainfall erosivity by
using 15-minute RTS in a mountain region in Michoacan state in Mexico.

On the global scale, the GloREDA database was built using data from almost 4000 weather stations worldwide (Panagos
et al., 2023), where 15 weather stations are widespread in the Mexican territory. They contain 5-minute RTS data from 2005 to
180 2015; however, not all the RTS have registers for the multiyear period of ten years. Indeed, some RTS have just four years of
registers. On the other hand, GloREDA provides monthly erosivity values in a raster format (.geotiff) (Figure 3a). We calculated
the rainfall erosivity of GloREDA database as the sum of the twelve raster files (one by month). We performed the verification
of our Mexico-CN3 and GloREDA dataset by comparing the mean and the standard deviation values by ecoregion.

At the national scale, Torres (1991) estimated rainfall erosivity using 54 RTS across Mexico (Figure 3b). The temporal
185 resolution for those 54 RTS is 1 minute, with a temporal period from 1977 to 1987. However, not all RTS have registers for
those ten years, so we selected 42 RTS presenting more than five years of registers. We will refer to this dataset as erosivity-
Cortés. Then, we adjusted a linear model using the R factor as the dependent variable and the multiyear mean rainfall as
the predictor variable. We adjusted those linear models with three datasets: erosivity-Cortés, Mexico-CN1, and Mexico-CN2
to compare the slope of the linear models. We mean-centered the predictor variable to shift its mean to zero, improving the
190 interpretability of the intercept.

At the local scale, the Michoacan mountain region has a database with 30 RTS (Figure 3c). These RTS have a 15-minute
temporal resolution, and the period of registers is from 2011 to 2017. The weather stations belong to the Association of
Producers, Packers, and Exporters of Avocado from Mexico (APEAM). For those RTS with more than five years of registers,
we estimated the rainfall erosivity R as the mean value of the annual erosivity R_y for the multiyear period. However, as finer
195 time resolution is available in this case, we estimated the rainfall erosivity $R(EI30)$ by rainfall event, as defined in Wischmeier
and Smith (1978) by using the `RainfallErosivityFactor` package (Cardoso et al., 2020) in R project. Afterward, we
aggregated the 15-minute RTS into daily totals by summing the values for each day. After we calculated rainfall erosivity as
described in section 2.2. As we calculated daily erosivity values using the adjusted parameters from Xie et al. (2016) we denoted
these rainfall erosivity values as $R(Xieetal.,2016)$. We identified the relationship between $R(EI30)$ and $R(Xieetal.,2016)$
200 by performing a linear regression. In this sense, the slope of the linear model quantifies the mean change of $R(EI30)$ when
 $R(Xieetal.,2016)$ increases a unit.

3 Results

This section presents the results of the three principal methodological stages outlined in the workflow. First, we developed
a daily-resolution rainfall time series database, which provided a basis for further analysis. Second, we estimated rainfall

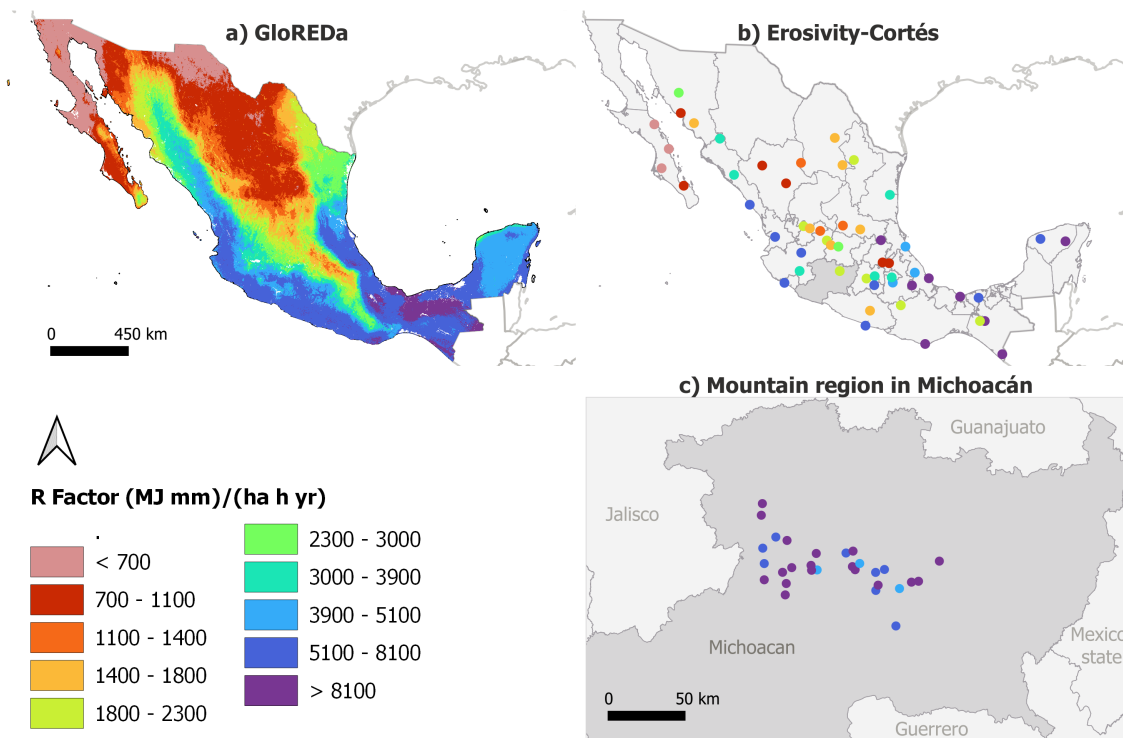


Figure 3. Spatial distribution of the validation datasets: a) GloREDA, b) Erosivity-Cortés, and c) Michoacan Mountain Region

erosivity values using a power law equation. Lastly, we verified these values by comparing them with global, national, and local databases.

3.1 Rainfall time series database development

The resulting database includes 1479, 1774, and 1721 RTS for CN1, CN2, and CN3, respectively (Table 1). The RTS with less than 20% of missing values and the identification of the number of series with NA and zero consecutive values are summarized in Appendix A3. After the data gap-filling, homogenization, and quality control processes, we discarded the 4.8% of the RTS. Hence, Table 1 shows that the largest number of RTS corresponds to CN1 (1968-1997), with 7.4% (109 RTS), which is followed by CN2 (1978-2007), with 5.4% (95 RTS) and CN3 (1988-2017), with 1.9% (33 RTS). Likewise, the most significant proportion of discarded RTS corresponded to Mediterranean California (3 RTS, 21.4%) and North American Deserts (29 RTS, 15.84%) in CN1; Mediterranean California (2 RTS, 11.11%) and Great Plains (7 RTS, 12.72%) in CN2; and Great Plains (5 RTS, 10.86%) in CN3. Additionally, in the data gap-filling processes, we identified that any of 5 RTS available for Mediterranean California had a rainfall register for three consecutive years; which did not allow us to carry out the data gap-filling process for the complete study period. Finally, the available number of RTS are 1370, 1676 and 1683 for CN1, CN2 and CN3, respectively. The available RTS are distributed across the Mexican territory for the three CNs and represent the seven ecoregions (Figure 4).



Table 1. Number of available rainfall time series before and after data gap-filling process, as well as the number of discarded rainfall time series. The frequency of rainfall time series (RTS) is shown by ecoregion and climate normal

Ecoregion	RTS before data gap-filling process			RTS with change greater than 10%			RTS after the data gap-filling process		
	1968-1997	1978-2007	1988 - 2017	1968-1997	1978-2007	1988 - 2017	1968-1997	1978-2007	1988 - 2017
Mediterranean California	14	18	5	3	2		11	16	
North American Deserts	183	273	243	9	18	4	154	255	239
Semi-arid Elevations	248	314	322	5	12	5	243	302	317
Great Plains	38	55	46	3	7	5	35	48	41
Tropical Rain Forest	195	237	236	6	6	3	179	231	233
Dry Forest	401	466	454	6	25	10	375	441	444
Temperate Sierras	400	411	415	27	25	6	373	386	409
Total	1479	1774	1721	109	95	33	1370	1679	1683

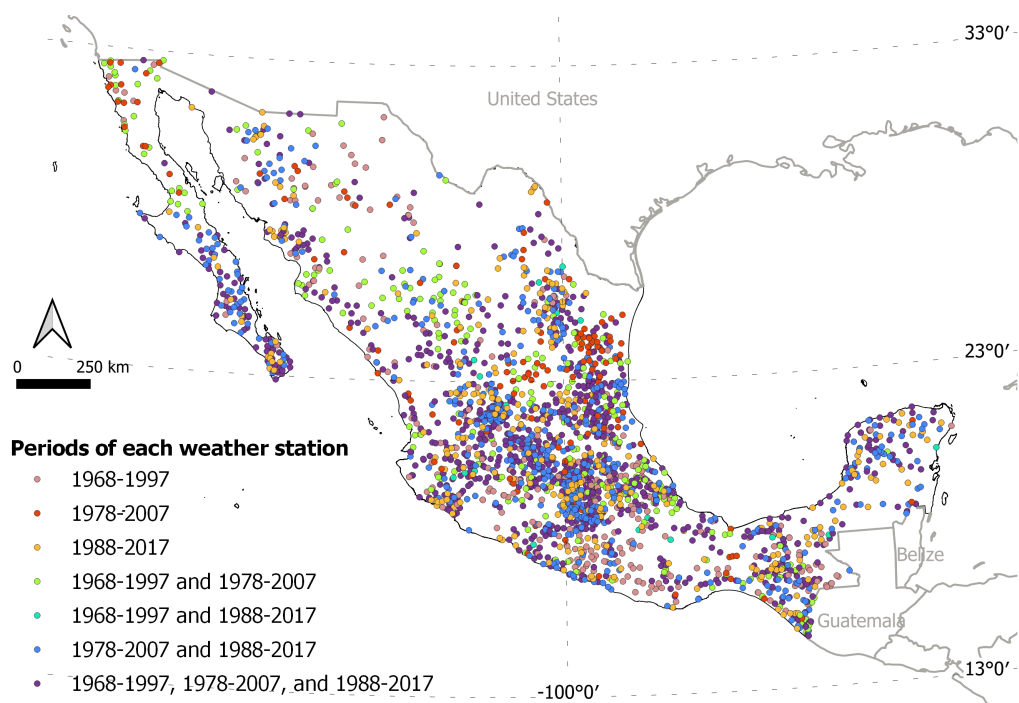


Figure 4. Spatial distribution of the weather stations

The percentage of variation of the series mean by ecoregion and CN using the two-step clustering is shown in Table 2. The CN 1978-2007 showed the highest average change in the mean, with -1.80%, where it is also noted that four of the seven ecoregions present relatively high averages changes. It is noteworthy that in CN 1968-1997, for North American Deserts, the highest average change in the mean is -1.50%. In the period 1988-2017, for Tropical Dry Forest and for Temperate Sierras,



it is -3.38% and -1.61%, respectively. Additionally, in A4 there is shown the Root Mean Square Error (mm) of the monthly accumulated rainfall by ecoregion. It can be seen that the highest RMSE was found for Tropical Rain Forest in the three CNs (6.12, 5.72, 6.78 mm, respectively), followed by Great Plains in CN2 and CN3 (5.72, 6.78 mm, respectively).

Table 2. Average percent (%) of change of the mean of rainfall time series by ecoregion

Ecoregion	Average change of the mean (%)		
	1968-1997	1978-2007	1988 - 2017
1 Mediterranean California	-0.84	3.24	
2 North American Deserts	-1.50	-1.36	-0.14
3 Semi-arid Elevations	-0.25	-1.37	0.03
4 Great Plains	-0.69	3.23	-0.29
5 Tropical Rain Forest	-0.06	0.20	0.10
6 Tropical Dry Forest	-0.54	-0.49	-3.38
7 Temperate Sierras	-0.20	-3.73	-1.61
Total	-0.28	-1.80	-0.98

Figure 5 shows the monthly rainfall distribution for the seven ecoregions for the multi-year period 1968-1997. In Appendix A1 is the monthly rainfall distribution for the period 1978-2007 and in the Appendix A2 is the monthly rainfall distribution for the period 1988-2017. Generally, rainfall is concentrated between May and November in ecoregions, except in Mediterranean California, where high values occur between November and April. For Mediterranean California, North American Deserts, Semi-arid Elevations and Great Planins, the rainfall does not exceed 200 mm for the month with the highest volume. However, the rainfall in Tropical Rain Forest, Tropical Dry Forest and Temperate Sierras can reach up to 800 mm in June and September. These general behavior of rainfall distribution by ecoregion is the same for the three CNs.

3.2 Rainfall Erosivity estimations

In this section, we will display the results of the estimations of the annual erosivity values for the three CNs studied. First, a descriptive statistic for erosivity values and their spatial distribution. Second, the identification of the erosive days.

The mean values for the three CNs expressed in $\text{MJ mm ha}^{-1} \text{ h}^{-1} \text{ yr}^{-1}$ were 3600 (SD 3748), 3296 (SD 3500), and 3461 (SD 3382), respectively (Table 3). The Krustal-Wallis test showed that the erosivity mean value for CN2 differed from CN1 and CN3 at a 95% confidence level. The coefficient of variation is around 1, which means significant variability. The statistical distribution of the erosivity values was right-skewed for the three CNs (skewness: 2.6, 2.9, 2.9, respectively), so the outliers are high erosivity values reaching more than $8000 \text{ MJ mm ha}^{-1} \text{ h}^{-1} \text{ yr}^{-1}$ for the three CNs (Figure 6).

Regarding the spatial distribution, the erosivity values across Mexican territory look similar for the three CNs. The ranges plotted in the legend correspond (not precisely) to the deciles of the three statistical distributions. In the California peninsula, there are concentrated those fewer erosivities (peach dots) with less than $700 \text{ MJ mm ha}^{-1} \text{ h}^{-1} \text{ yr}^{-1}$, which represents the 1st decil of the distribution. The 2nd decil (values between 700 and $1100 \text{ MJ mm ha}^{-1} \text{ h}^{-1} \text{ yr}^{-1}$) is concentrated in the northern

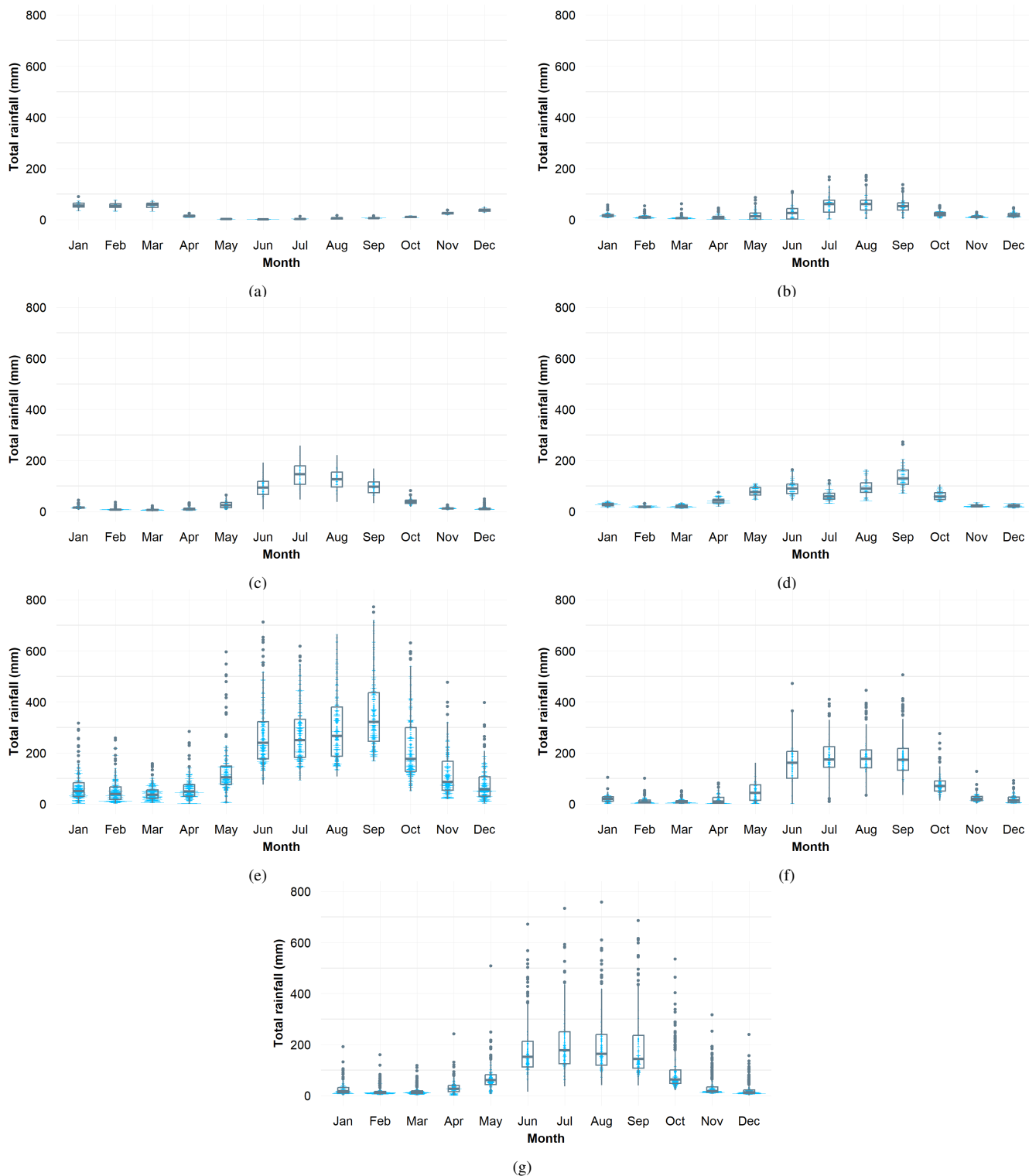


Figure 5. Mean monthly rainfall for each ecoregion for the climate normal 1968-1997. a) Eco 1, b) Eco 2, c) Eco 3, d) Eco 4, e) Eco 5, f) Eco 6, and g) Eco 7.



Table 3. Descriptive statistic of the erosivity values for three climate normals (1968-1997, 1978-2007, 1988-2017). Min: minimum, Max: maximum, SD: standard deviation, CV: coefficient of variation, skew: skewness, kurt: kurtosis

Climate normal	n	Mean	SD	Min	Max	CV	Skew	Kurt
1968-1997	1369	3600a	3748	48.0	31946.0	1.0	2.6	12.2
1978-2007	1678	3296b	3500	39.0	29330.0	1.1	2.9	15.0
1988-2017	1676	3461a	3382	47.0	28812.0	1.0	2.9	15.0

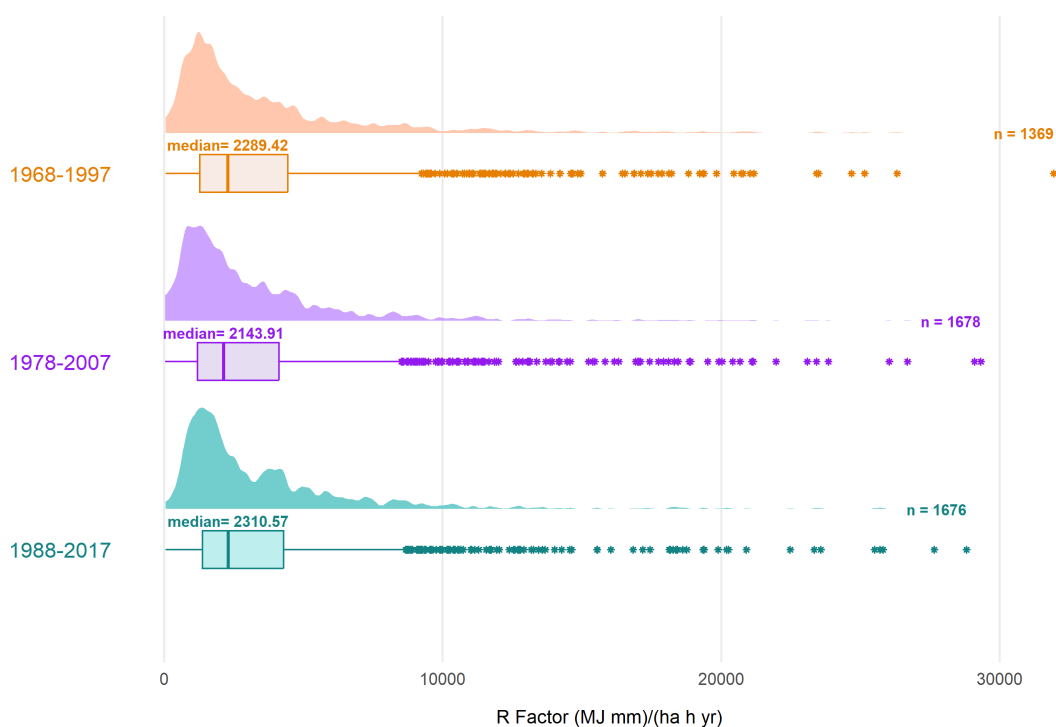


Figure 6. Density plot and Box-Plot of erosivity factor (R) calculated from daily rainfall time series for the three climate normals

245 and extends a little to the central region (red dots). These areas represent the North American deserts and Semiarid elevations
 ecoregions. On the other hand, the 9th (dark blue dots) and 10th (dark purple dots) with values between 5000 to 8100 and
 greater than 8100 MJ mm ha⁻¹ h⁻¹ yr⁻¹, respectively, are concentrated in the tropical rain forest ecoregion in the southwest
 region, and some places in the tropical dry forest ecoregion in the southeast of Mexico. It is clear that for the CN3 (1988-
 250 the rainfall series there had records until 2012.

The erosive days were considered as those with rainfall greater than 12.5 mm. Figure A3 shows the mean number of locations
 with erosive rain for each day of the year. For the three CNs, there is one erosive period throughout the year; however, for CN3



the erosive period is marked by two peaks, first from day 173 to 190 and second from day 229 to 261; these days represent those with the most (10% higher) locations reporting erosive rainfall. On the other hand, the 90-decile number of locations with erosive rainfall for CN2 and CN3 has increased by 7% (238) and 12% (227) concerning CN1 (212).

3.3 Verification of Rainfall Erosivity

In this section, we present the verification results of the usability of the national dataset of precipitation series at daily resolution. To achieve this, we compared the erosivity values of our datasets, called Mexico-CN3 and Mexico-CN2, with a global database (GloREDA), a national database (Erosivity-Cortés), and a local database (Erosivity-Michoacan) (Figure 8).

Using Mexico-CN3 and GloREDA datasets, we compared the mean values for six ecoregions (Figure 8a). Tropical rainforests, temperate Sierras, and the Great Plains are the ecoregions with more significant differences between means. Comparing Mexico-CN3 concerning GloREDA, there is an overestimation for Tropical Rain Forest and Great Plains, and for temperate Sierras, there is an underestimation. On the other hand, North American Deserts, Semi-arid Elevations, and Tropical Dry Forest ecoregions have very similar erosivity mean values. The reader must remember that CN3 (1988-2017) has no available precipitation series in the Mediterranean California ecoregion.

At the national scale, comparing our datasets (Mexico-CN1 and Mexico-CN2) with the erosivity-Cortés, we identified that Mexico-CN1 and Mexico-CN2 well represent the relationship between R and multi-year average annual rainfall (Figure 8b). When adjusting a linear model using R as the dependent variable and the multi-year average annual rainfall as the predictor, we can find that the coefficients of the predictor variable are very similar, 5.95, 5.47, and 5.41, for erosivity-Cortés, Mexico-CN1 and Mexico-CN2, respectively. The intercepts (calculated with the predictor variable centered) are 3738, 3600, and 3296 for erosivity-Cortés, Mexico-CN1, and Mexico-CN2, respectively. The variance explained for each model is 0.64, 0.9, and 0.9 for erosivity-Cortés, Mexico-CN1, and Mexico-CN2, respectively.

At the local scale, the calculated $R(EI30)$ is greater concerning $R(Xieetal., 2016)$ as shown in Figure 8c. The coefficient for $R(Xieetal., 2016)$ is 1.82 (p-value 8.18e-10); The intercept is 8945 MJ mm ha⁻¹ h⁻¹ yr⁻¹ (p-value 2e-16); and the variance explained by the linear model is 84.7%. It is clear that the $R(Xieetal., 2016)$ values are underestimated compared with $R(EI30)$ when using Erosivity-Michoacan dataset.

4 Discussion

This research addressed the data incompleteness and breakpoints present in the available Mexican climate time series, resulting in a comprehensive and unprecedented database of rainfall time series. The new information is primarily applicable to the analysis of rainfall erosivity required for studying soil erosion at the national scale of Mexico. The new information is appealing for diverse users, as the insufficient availability of climate information (i.e., publicly funded data), it represents an interoperability barrier limiting the development of climate services and the understanding of key ecosystem climate-related processes at different scales (Vaughan et al., 2016). Consequently, scientists search for new ways to create national climate-related datasets containing state-of-the-art information for a diverse range of applications such as climate modeling, yield prediction, or eco-



285 logical forecasting. Particularly, we compiled and systematized a national dataset with daily rainfall and rainfall erosivity for
three climate normals (1968-1997, 1978-2007, and 1988-2017) across Mexico. To the best of our knowledge, this research is
the first effort to develop a large daily RTS dataset based on legacy climate data at the national scale.

We also address the data incompleteness and breakpoints that exist in Mexican climate time series available data, as indicated
in previous reports (Cuervo-Robayo et al., 2020). The new information ensures the highest possible quality, (as explained
290 in the methods section) it includes a rigorous quality control, homogenization, and data gap-filling procedures of around
4000 daily RTS: 1370, 1679, and 1683 RTS for the CNs 1968-1997, 1978-2007, and 1988-2017, respectively. At the national
scale, other extensive studies have been conducted, but they use a coarser time resolution compared to that studied here. For
example, Cuervo-Robayo et al. (2014) updated the mean monthly rainfall for 100 years (1910-2009) using around 5000 RTS.
Studies compare multiple gap-filling approaches at a regional scale (Cespedes et al., 2023) and conduct quality control and
295 homogenization process (García-Cueto et al., 2019) using daily RTS. Yet, those studies use RTS datasets representing shorter
periods of time compared to our study. Studies using RTS across comparable periods of time to our study consider RTS
with fewest missing data, without considering a data gap-filling process Pineda-Martínez and Carbajal (2017); Mateos et al.
(2016). Thus, our research represents a significant contribution by offering a more comprehensive and higher-quality daily RTS
dataset, addressing limitations related to the dataset size, representativeness, and the rigorous process of homogenization and
300 data gap-filling. We contribute with a new standard for climate data analysis at the national scale in Mexico.

Our methodology allowed us to reconstruct climate series with significant missing data gaps, as reported in previous studies
(Guijarro, 2014). The methodology applied on an ecoregion basis, potentially increases spatial coherence in the completed and
homogenized RTS, as previously recommended (Adeyeri et al., 2022). The methodology is also recommended by the World
Meteorological Organization (World Meteorological Organization, 2020). Other robust data gap-filling strategies leverage high
305 computational capacity and big data analyses (i.e., machine learning) to obtain reliable RTS (Hirca and Türkkan, 2024; Lupi
et al., 2023). These strategies build a predictive function to estimate values for missing data using the climate series data itself
or auxiliary data such as satellite products (Duarte et al., 2022). Despite the performance predicting missing data values (Hirca
and Türkkan, 2024; Lupi et al., 2023), many machine learning methods are still experimental, and a well-known and WMO-
recommended methodology (as a reference point) is needed to benchmark more complex data-driven approaches. We recognize
310 that our effort is not error free, and therefore we present an estimation of error in our gap-filling approach in supplementary
material A4. Future improvements of this new RTS database must include a progressive exploration of multiple gap-filling data
techniques.

The gap-filled dataset (considering the completed and homogenized RTS for the three CNs) is useful for analysis of changes
in precipitation trends (Yan et al., 2014) across Mexico. This new RTS dataset shows that the regional variation in rainfall
315 patterns is markedly latitudinal (Figure 5 and Appendix A1 and A2), from Tropical Rain Forests across the south east, to the
water limited environments of North American Deserts. These results are consistent with rainfall patterns previously reported
by de Anda Sánchez (2020). In addition, the new dataset also provides an earlier perspective of the rainfall erosivity spatial
distribution in Mexican territory.



Our work reveals that the distribution of erosivity values in Mexico corresponds to the geographical distribution of the rainfall and seasonal rainfall conditions. The areas with the major erosivity values are concentrated in the isthmus of Tehuantepec (i.e., the shortest distance between the Gulf of Mexico and the Pacific Ocean), where the highest mean annual rainfall values in Mexico have also been reported (de Anda Sánchez, 2020). In contrast, lower erosivity values are in Mexico's central and northern regions, where severe droughts (e.g., that from the 1990s until the beginning of the twenty-first century), due to the large-scale changes in ocean-atmospheric circulation patterns, have affected the mean annual rainfall. On the other hand, we highlight a spot in the south of the California peninsula (e.g., Sierra La Laguna), where erosivity values are higher than those estimated in the north. This local variation is due to the influence of tropical cyclones, which contribute up to 50% of the mean annual rainfall in this region (Agustín Breña-Naranjo et al., 2015). Overall, the spatial variability in erosivity across Mexico reflects the interplay between rainfall patterns and climatic events, underscoring the significant influence of regional weather phenomena on soil erosion processes.

The new dataset is appealing for validating global datasets. Comparing the new dataset with GloREDA, we identified that the mean values of rainfall erosivity for North American Desserts, Semi-arid Elevations, and Tropical Dry Forest ecoregions are similar in more than 50% of the Mexican area. In contrast, those ecoregions with higher annual rainfall such as the Tropical Rain Forest, show differences compared to GloREDA. This difference is evident because the ecoregion has higher mean annual rainfall and standard deviation (862 to 4823 mm and an SD of 758 mm). In comparison, the GloREDA data set reports a lower mean annual rainfall (1383-2100 mm and an SD of 402.35 mm, those values calculated with three RTS in the ecoregion). The same pattern is observed for Temperate Mountains where Mexico-CN3 has a wider probability distribution of mean annual rainfall (range of 318-4009 mm and an SD 500 mm) than GloREDA (range of 814 to 2258 mm, in this ecoregion GloREDA has just two RTS). We therefore report a more complete description of RTS variance compared with that in GloREDA. We believe that our contribution could be useful to better represent global erosivity estimates.

Aligned with our results, Fenta et al. (2023) found the largest differences in annual rainfall erosivity values between the GloREDA database and a satellite-based approach (using sub-hourly RTS) for the rainiest regions (tropical and temperate climates) around the world. The best agreement between satellite-based rainfall erosivity (using the satellite precipitation estimates corrected and reprocessed with the Climate Prediction Center Morphing Technique - CMORPH) and interpolated GloREDA (Panagos et al., 2017) was found in Europe, where the density of rainfall gauges is the highest globally (Bezák et al., 2022). Furthermore, with just 15 rainfall gauges in Mexico, it is important to identify the regions with high discrepancies between national approach and interpolated GloREDA, in order to understand their limitations and use them in places with scarce rainfall erosivity information.

At the national scale, we observe a general underestimation of erosivity values compared with the erosivity-Cortés dataset, which is evident in the intercepts of the linear models (Figure 8b). Although calculated at a coarser temporal resolution, this pattern has already been indicated by Tu et al. (2023); Yin et al. (2015) while evaluating the effect of modifying the time interval for calculating $R(EI30)$ using 5, 15, 30, and 60-minute RTS. The authors concluded that increasing the time interval leads to underestimating erosivity values. Similarly, Li et al. (2022) identifies that using a monthly model underestimates $R(EI30)$. However, the same author found an overestimation of the R values regarding $R(EI30)$ using annual models. Therefore, having



more detailed information is arguably the best way to estimate the erosivity factor with greater certainty and to know which
355 model explains the greatest variance of $R(EI30)$. Our results highlight the advantage of having detailed information for the
mountain region in Michoacan.

Comparing our results with the erosivity-Michoacan dataset $R(EI30)$ based on a 15-minute RTS with the R calculated
from Xie et al. (2016), we observe that for every unit change in R with Xie's equation, the $R(EI30)$ is 1.85 times larger. This
can be seen in the slope of the linear model in Figure 8c. The adjustment coefficient applies only to the rainfall conditions
360 of the mountain region in Michoacan. For other areas, it has been shown that the fit of a model is not the same for different
rainfall patterns Li et al. (2022). Furthermore, this adjustment may not be applicable across all Mexican territories. Additionally,
although Xie's model has been tested for other hourly data sets and good results have been obtained (CC=0.96, NSE=0.91, and
BIAS=-1-11%), it is still recommended to use the data with the finest temporal resolutions, especially for those regions with
smaller amounts of rainfall (Chen et al., 2020). In Mexico the smaller amounts of rainfall fall in the ecoregions of California
365 Mediterranean, North American Deserts, and the Great Plains.

As potential limitations to this study, we selected just one methodology for gap-filling daily data. Multiple remote sensing
products could help to improve gap-filling efforts. These products include the Climate Hazards Group InfraRed Precipitation
with Station data (CHIRPS) (Funk et al., 2015) with daily temporal resolution; the National Oceanic and Atmospheric Ad-
ministration (NOAA) data presenting hourly time resolution, and Climate Prediction Center Morphing Technique (CMORPH),
370 among others. Using various data sources improves the robustness of the resulting datasets (Bessenbacher et al., 2023) because
those products enhance the completeness of the RTS and the accuracy of the gap-filling data. On another hand, the selection of
the model for calculating erosivity is a source of uncertainty in subsequent models estimating soil loss rates (Li et al., 2022).
Therefore, evaluating the performance of different adjusted models is appealing for future research when high-resolution time
series data are available. Additionally, at the national scale, it is important to test other daily models and estimate the variation
375 of the predictions by ecoregions. Additionally, if finer RTS were available for the entire national territory, it would be possible
to calibrate a potential equation for Mexico.

The new database is a potential tool for local, national and global erosion studies. At the local scale this database could serve
as a tool to design field experiments to validate rainfall erosivity estimations in different rainfall patterns, as well as to identify
the magnitude of the underestimations or overestimation when using different time-resolution of the RTS (Meng et al., 2021;
380 Zhao et al., 2019; Dunkerley, 2019). At the national scale, this database could serve as input in erosion models to generate a
base line of soil loss rates across Mexican territory. This necessity have been highlighted in Bolaños González et al. (2016).
The authors emphasize the necessity to estimate soil and organic carbon loss rates. Additionally, this could help to support
the development of environmental monitoring systems in Mexico. At the global scale, the results could serve as validation
benchmarks and increase the representativeness of global rainfall erosivity database such as GloREDa (Panagos et al., 2023)
385 or the Global Rainfall Erosivity database from Reanalysis and Satellite Estimates -GloRESatE- (Das et al., 2024). The new
information is appealing for the aforementioned efforts as Mexican territory does not have enough data representation due to
the lack of primary information. The new dataset and their possible improvements would allow for a more accurate estimation



of erosivity and, thus, the annual amount of soil lost due to rainfall. This implies a better understanding of soil resources, better territorial planning, better agricultural and land use management, and better land conservation programs.

390 **5 Conclusions**

We present an unprecedented rainfall erosivity database across Mexico. The research used legacy climate data to achieve erosivity across Mexican territory. However, the rainfall time series (RTS) contained a relatively large number of missing values. In order to increase RTS completeness, a gap-filling procedure was performed to obtain gap-free estimates for three climate normals. The new database let provide a more detailed insight of rainfall erosivity respect to global models. This study reveals that
395 the North American deserts and Mediterranean California are regions where the rainfall has less erosive power, while tropical rainfall forests have the highest rainfall erosivity. The new database is available for public consultation. This database is for researchers and students, technical assistants, decision-makers, and others users interested in rainfall erosivity patterns and trends. Additionally, all environmental studies in Mexico, where the rainfall process is needed at the daily resolution, may benefit from this dataset.

400 **6 Code availability**

Rproject scripts to reproduce the workflow described in this research is available at: <https://zenodo.org/records/13830947> (Varón-Ramírez, 2024)

7 Data availability

Following the FAIR principles for scientific data, we published our resulting databases (Mexico-CN1 1968-1997, Mexico-
405 CN2 1978-2007, and Mexico-CN3 1988-2017) and the completed daily rainfall time series for the three climate normals in the Environmental Data Initiative (EDI) at <https://doi.org/10.6073/pasta/7479676e406aeb40127da7b096b28eb2> (Varón-Ramírez et al., 2024).

Rainfall erosivity databases contain eleven columns with the weather station location (code, coordinates, altitude, name, and ecoregion), the root means squared error (RMSE) of the data gap-filling process, rainfall erosivity, the accumulated number of
410 days with erosive rainfall, and the multiyear mean rainfall.

Daily rainfall time series databases contain 1369, 1678, and 1676 columns for the climate normal 1968-1997, 1978-2007, and 1988-2017, respectively. Each column corresponds to one rainfall time series.

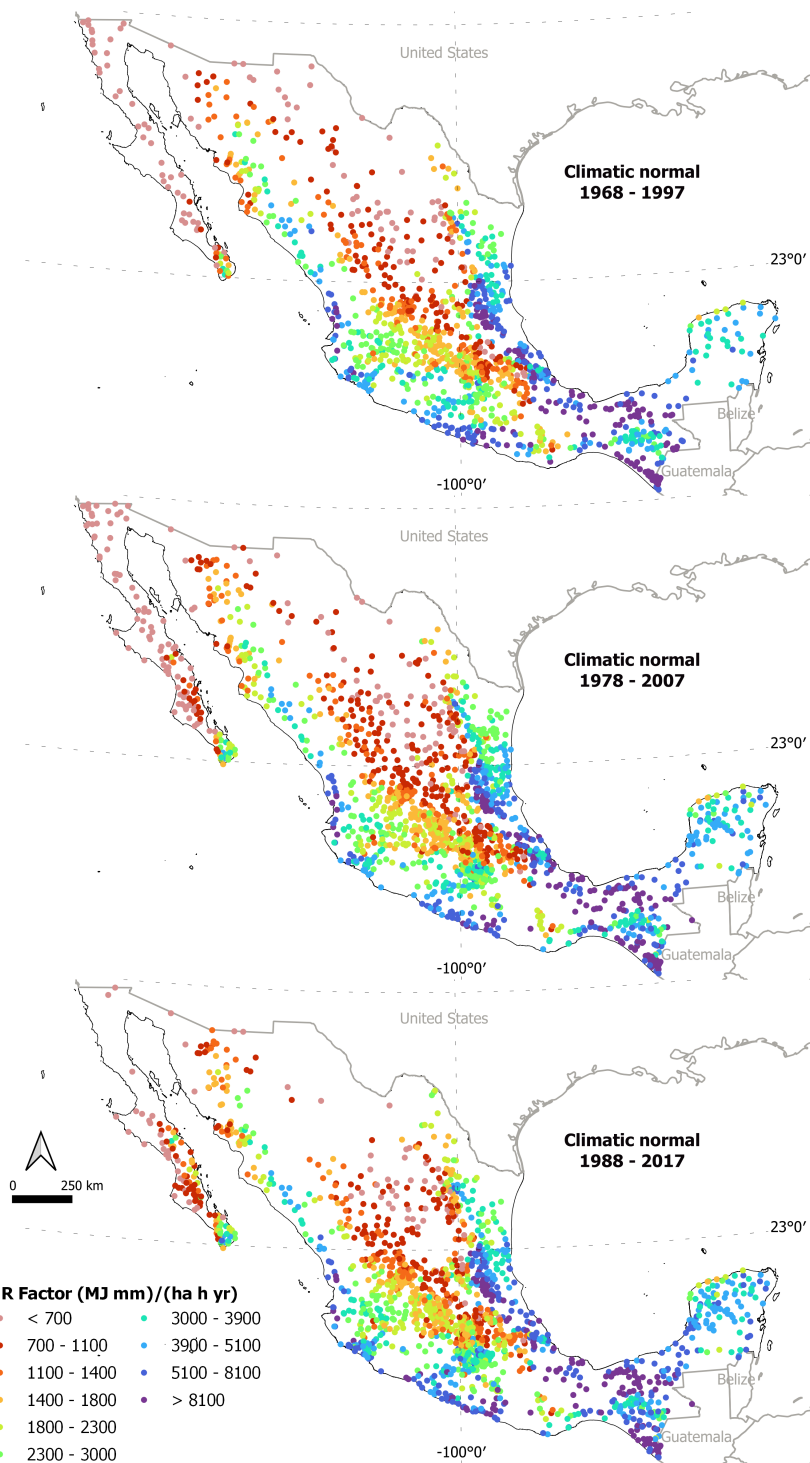


Figure 7. R factor values calculated with the power law equation proposed by (Xie et al., 2016) at daily resolution for three climate normals

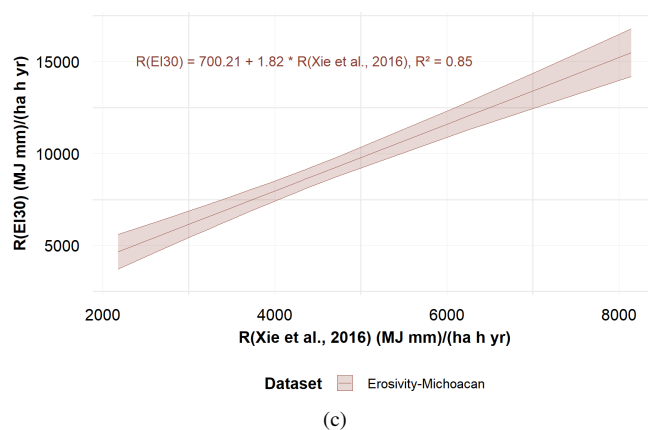
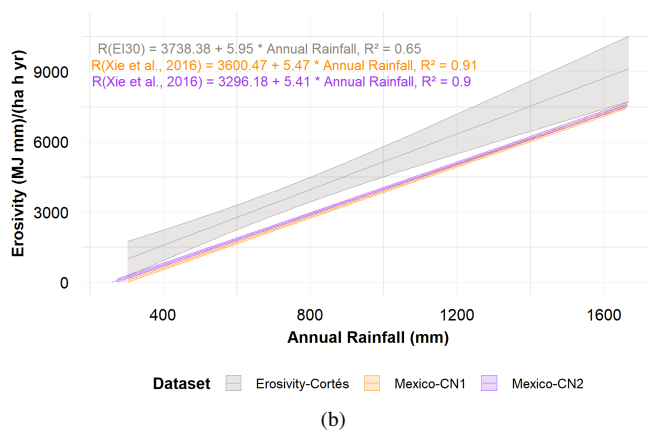
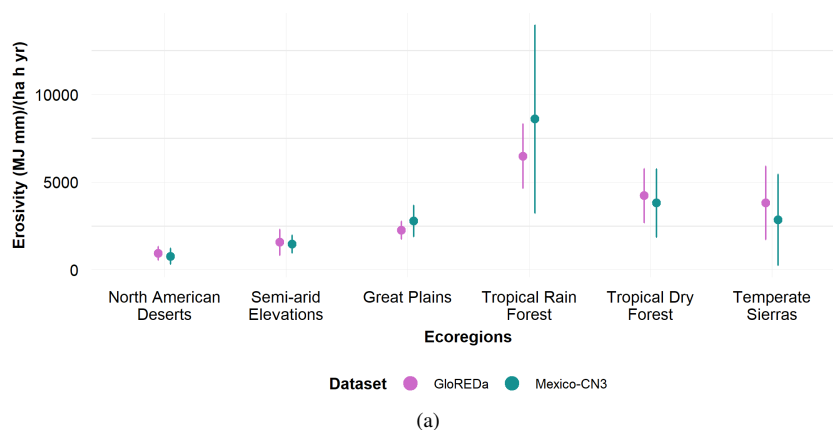


Figure 8. Verification of rainfall erosivity datasets (Mexico-CN1, Mexico-CN2, and Mexico-CN3) with three erosivity databases at different scales (global, national and local). a) Global verification: Comparison of mean values of rainfall erosivity from GloREDA and Mexico-CN3 datasets in six ecoregions of Mexico. b) National verification: Comparison of rainfall erosivity values from Erosivity-Cortés, Mexico-CN1, and Mexico-CN2 by performing a linear regression model using annual rainfall (mm) as predictor. c) Local verification: Linear regression model using rainfall erosivity values, R(EI30) and R(Xie et al.2016), using RTS (from Erosivity-Michoacan dataset) at two temporal resolutions, 15-minute and daily resolution, respectively.



Appendix A

A1 Homogenization parameters for monthly rainfall time series

Table A1. Homogenization parameters for monthly series. Eco: Ecoregion (1: Mediterranean California, 2: North American Deserts, 3: Semi-arid Elevations, 4: Great Plains, 5: Tropical Rain Forest, 6: Tropical Dry Forest, 7: Temperate Sierras); dz.max and dz.min (upper and lower): standard deviations to consider suspicious and anomalous data

Climate normal	Ecoregion	inht	dz.max	dz.max	dz.min	dz.min
			lower	upper	lower	upper
1968 - 1997	1	15	8	10	-8	-10
	2	25	12	13	-7	-8
	3	40	10	11	-8	-9
	4	20	6	7	-5	-6
	5	30	8	9	-6	-7
	6	30	14	16	-10	-10
	7	35	12	13	-7	-8
1968 - 1997	1	15	10	10	-10	-10
	2	35	12	13	-8	-9
	3	35	11	12	-8	-9
	4	20	8	9	-7	-8
	5	50	8	9	-7	-8
	6	30	13	14	-10	-11
	7	40	9	10	-8	-8
1968 - 1997	1	–	–	–	–	–
	2	50	14	14	-10	-10
	3	60	14	14	-8	-8
	4	15	7	7	-6	-6
	5	55	8	8	-7	-7
	6	60	14	14	-10	-10
	7	100	12	12	-8	-8



415 A2 Homogenization parameters for daily rainfall time series by ecoregion and subgroup

Table A2. Homogenization parameters for daily rainfall time series by ecoregion and group. Eco: Ecoregion (2: North American Deserts, 3: Semi-arid Elevations, 5: Tropical Rain Forest, 6: Tropical Dry Forest, 7: Temperate Sierras); RS: Number of rainfall time series; inht: ; dz.max and dz.min (upper and lower): standard deviations to consider suspicious and anomalous data

1968-1997								1978-2007								1988-2017							
Eco	Group	RS	inht	dz.max lower	dz.max upper	dz.min lower	dz.min upper	Eco	Group	RS	inht	dz.max lower	dz.max upper	dz.min lower	dz.min upper	Eco	Group	RS	inht	dz.max lower	dz.max upper	dz.min lower	dz.min upper
2	1	94	50	40	45	-20	-20	2	1	142	60	32	34	-18	-18	2	1	112	100	40	45	-20	-25
	2	18	25	40	45	-25	-30		2	23	20	45	50	-25	-25		2	12	10	35	40	-25	-30
	3	36	20	40	45	-25	-30		3	68	12	35	40	-30	-35		3	45	20	35	40	-20	-25
	4	35	20	35	40	-20	-25		4	40	12	30	35	-20	-25		4	67	50	45	40	-30	-35
3	1	34	25	24	26	-10	-12	3	1	41	30	22	24	-12	-14	3	1	115	60	26	28	-16	-16
	2	87	40	26	28	-14	-16		2	55	25	22	24	-14	-14		2	27	20	22	24	-14	-14
	3	59	40	22	24	-12	-12		3	130	50	24	26	-14	-14		3	180	40	26	28	-18	-18
	4	52	40	26	28	-14	-14		4	71	40	24	26	-12	-14		1	80	60	22	24	-20	-22
	5	16	40	26	28	-10	-12		5	16	30	22	24	-10	-12		2	81	40	24	26	-16	-18
5	1	36	20	30	35	-15	-20	5	1	42	40	30	35	-25	-30	6	3	75	100	24	26	-16	-18
	2	11	5	20	22	-10	-10		2	13	50	18	20	-10	-12		1	290	200	35	40	-25	-30
	3	36	50	24	26	-14	-14		3	30	40	18	20	-12	-14		2	46	20	30	35	-20	-25
	4	58	50	30	32	-14	-16		4	32	40	18	20	-16	-18		3	85	80	35	40	-30	-35
	5	27	40	20	22	-10	-12		5	68	50	22	24	-16	-18		4	33	15	40	45	-35	-40
	6	27	40	20	22	-12	-14		6	52	30	20	22	-12	-14		1	242	250	26	28	-14	-14
6	1	118	25	35	40	-30	-30	6	1	62	20	30	30	-20	-25	7	2	59	100	35	40	-25	-25
	2	187	60	40	45	-25	-30		2	267	80	30	35	-25	-30		3	114	200	30	35	-25	-30
	3	77	25	40	40	-20	-25		3	117	25	30	30	-25	-30								
	4	19	25	50	55	-30	-35		4	20	10	40	45	-35	-35								
7	1	82	50	22	24	-14	-16	7	1	87	60	20	22	-12	-14								
	2	49	50	35	35	-20	-25		2	62	60	35	40	-25	-30								
	3	153	50	35	35	-25	-25		3	157	80	26	28	-12	-14								
	4	116	50	24	26	-10	-12		4	105	70	26	28	-22	-24								



A3 NA and zero values sequences identification

Table A3. Identification of number of rainfall time series with consecutive zero and NA values

Consecutive years	Number of RS with sequences of NA and zeros			Decision
	1968 - 1997	1978 - 2007	1988 - 2017	
1	794	787	611	Not changed
2	344	478	613	Not changed
3	155	286	277	Replaced with NA and used as reference
4	88	136	109	Replaced with NA and used as reference
5	77	78	82	Replaced with NA and used as reference
6	21	11	31	Replaced with NA and used as reference
7	1	1	0	Removed
8	2	0	1	Removed
9	1	2	2	Removed
10	2	0	0	Removed
11	3	2	1	Removed
12	0	0	0	Removed
13	0	1	1	Removed
14	0	1	0	Removed
15	0	0	0	Removed
16	1	2	0	Removed
RS (NA menor 20%)	1489	1785	1728	
RS removed	10	9	5	
RS for data gap-filling process	1479	1776	1723	



A4 Root Mean Square Error (mm) of the data gap-filling process for the monthly rainfall in the seven ecoregions

Table A4. Root Mean Square Error (mm) of the data gap-filling process by month and ecoregion. Eco: Ecoregion (1: Mediterranean California, 2: North American Deserts, 3: Semi-arid Elevations, 4: Great Plains, 5: Tropical Rain Forest, 6: Tropical Dry Forest, 7: Temperate Sierras)

Climate Normal	Eco	Jan	Feb	Mar	Apr	May	Jun	Jul	Aug	Sept	Oct	Nov	Dec	Total
1968-1997	1	6.84	6.71	6.10	1.36	0.33	0.16	0.67	0.58	0.60	0.78	1.74	3.43	2.44
	2	1.91	1.39	1.02	1.31	1.37	2.20	6.32	3.42	3.55	2.84	1.11	2.41	2.40
	3	1.83	0.96	0.93	0.78	1.42	3.08	3.64	3.15	3.06	1.85	0.74	0.83	1.86
	4	1.72	2.08	1.06	2.25	2.66	3.61	1.74	4.40	3.75	2.62	1.02	1.63	2.38
	5	3.07	3.57	4.28	3.20	6.06	7.92	8.39	8.45	9.79	8.32	5.66	4.78	6.12
	6	2.47	1.17	1.49	1.46	2.75	6.26	6.76	5.84	7.13	3.90	2.34	1.89	3.62
	7	2.31	1.07	1.53	2.06	2.75	4.55	5.11	5.00	8.03	3.93	2.11	2.06	3.38
1978-2007	1	8.16	5.81	7.87	1.63	0.86	2.53	0.41	1.40	0.70	1.73	3.27	5.69	3.34
	2	2.13	1.13	0.86	1.38	1.73	1.98	5.26	3.95	3.84	2.10	1.06	2.28	2.31
	3	1.66	0.93	0.75	0.72	1.38	3.54	3.73	3.21	3.49	1.81	0.75	0.95	1.91
	4	2.77	1.95	1.97	3.44	3.27	5.06	6.15	5.68	9.01	5.08	1.55	3.40	4.11
	5	4.04	3.82	3.15	3.02	6.01	7.71	6.34	7.07	8.66	9.14	5.22	4.51	5.72
	6	3.19	1.12	0.92	1.68	2.89	6.83	5.71	5.71	8.58	4.85	2.38	2.38	3.85
	7	2.37	1.31	1.17	2.35	4.08	5.61	6.34	5.54	6.92	6.92	2.72	2.27	3.97
1988-2017	2	1.59	1.45	2.08	1.11	2.02	2.14	6.21	3.96	4.88	2.53	1.89	2.69	2.71
	3	1.67	1.68	1.23	0.77	1.41	3.23	4.29	4.56	3.21	1.99	1.05	1.11	2.18
	4	2.75	2.53	4.08	6.08	8.74	5.68	13.17	9.87	12.52	6.27	5.05	6.27	6.92
	5	5.25	3.48	3.21	3.42	6.81	7.79	8.51	9.69	9.06	12.11	7.34	4.73	6.78
	6	3.56	1.68	1.57	2.38	3.48	6.35	6.55	6.78	8.28	5.42	2.41	2.36	4.24
	7	2.73	2.28	2.55	2.21	6.34	6.79	8.65	7.59	8.34	6.08	4.37	3.20	5.09
	Total		3.10	2.31	2.39	2.13	3.32	4.65	5.70	5.29	6.17	4.51	2.69	2.94



A5 Monthly rainfall distribution for two climate normals (CNs) 1978-2007 and 1988-2017

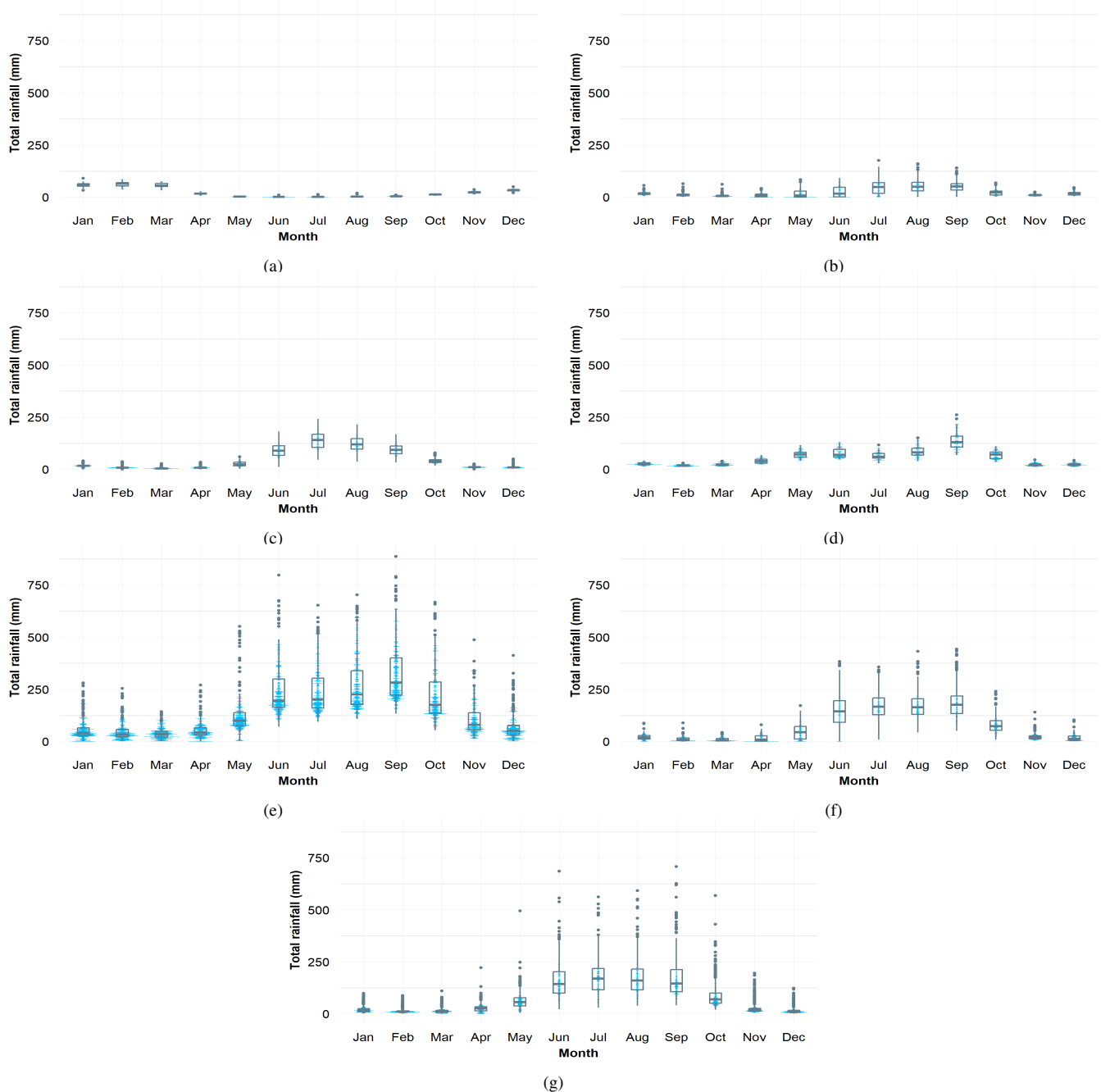


Figure A1. Mean monthly rainfall for each ecoregion for the climate normal of 1978-2007. a) Mediterranean California, b) North American Deserts, c) Semi-arid Elevations, d) Great Plains, e) Tropical Rain Forest, f) Tropical Dry Forest, g) Temperate Sierras

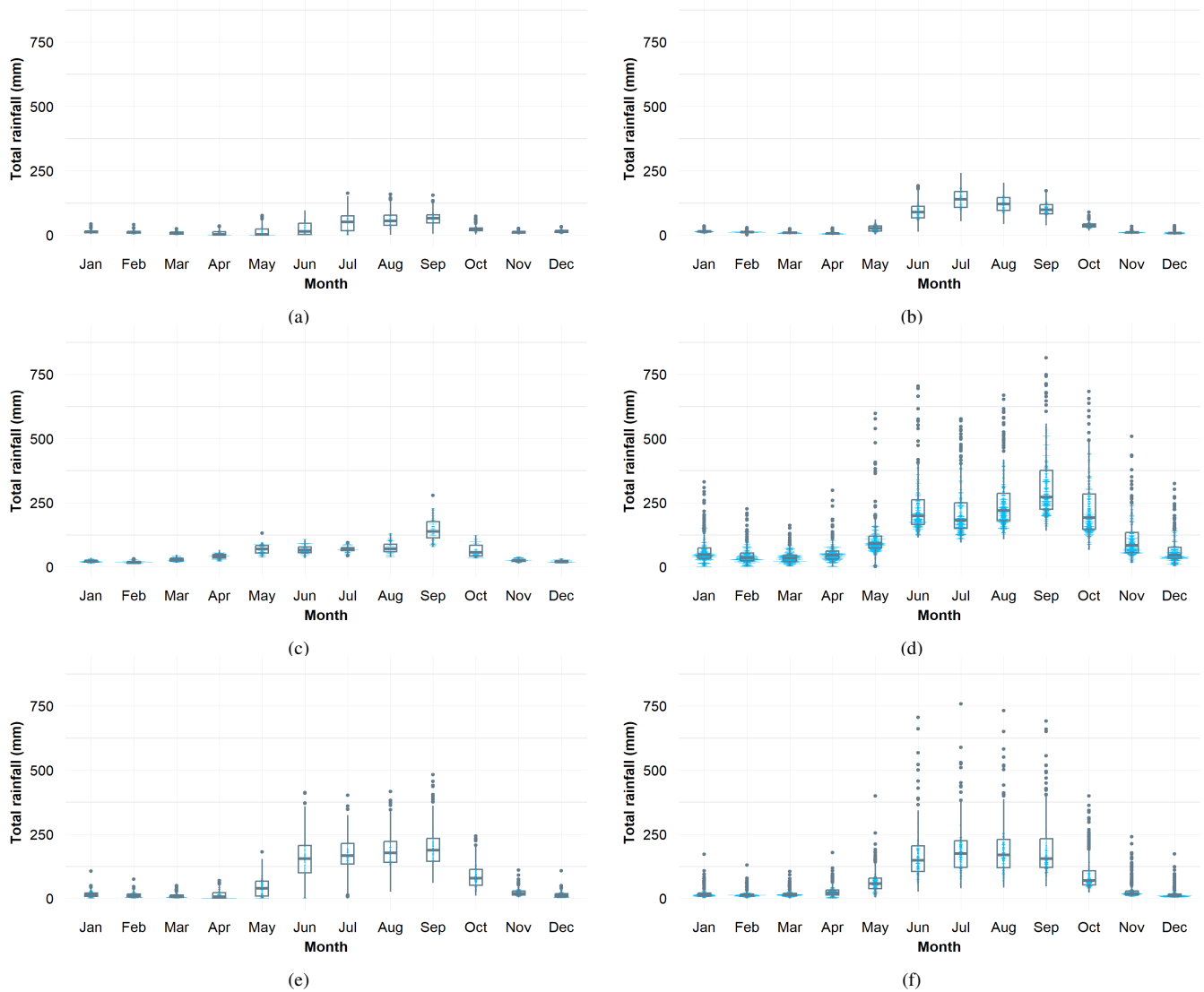
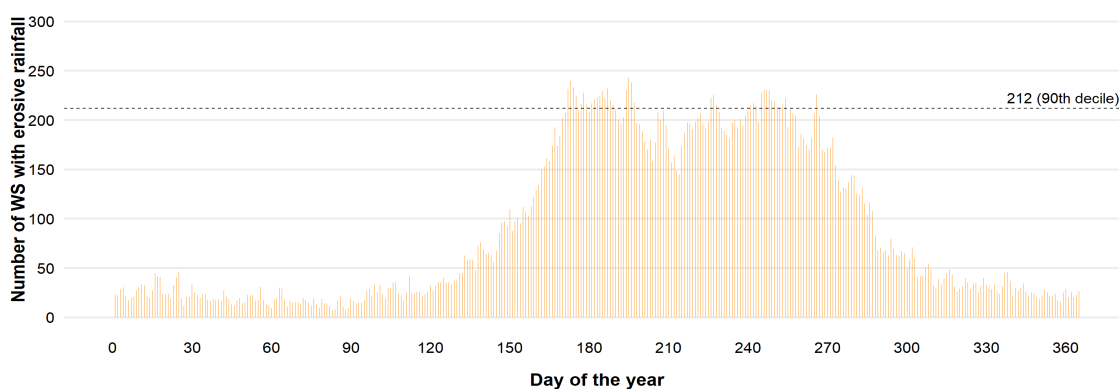


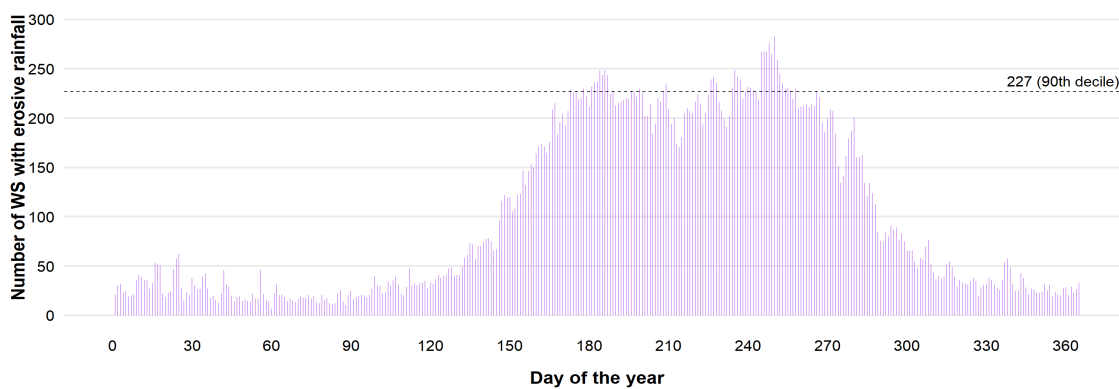
Figure A2. Mean monthly rainfall for each ecoregion for the climate normal of 1988-2017. a) North American Deserts, b) Semi-arid Elevations, b) Great Plains, d) Tropical Rain Forest, e) Tropical Dry Forest, f) Temperate Sierras



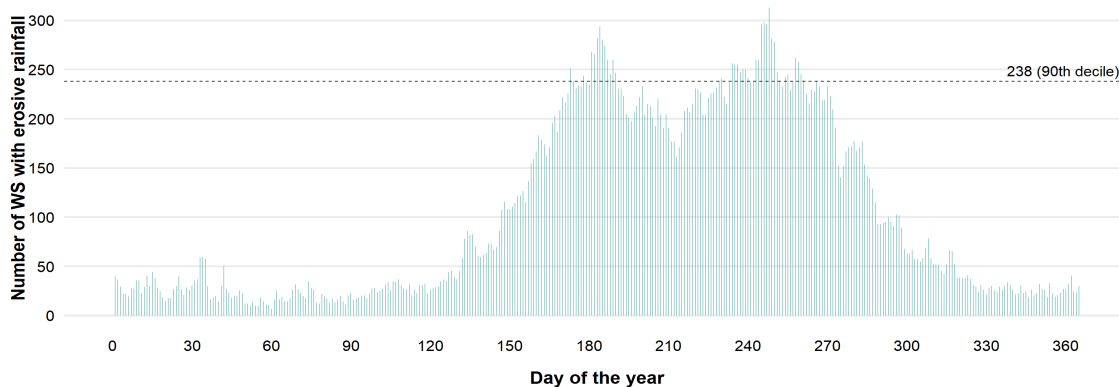
A6 Annual distribution of the number of locations with erosive rainfall



(a)



(b)



(c)

Figure A3. Number of locations with erosive rainfall of each day of the year for the three climate normal, a) 1968-1997, b) 1978-2007, and c) 1988-2017



420 *Author contributions.* Varón-Ramírez, Gómez-Latorre, and Guevara contributed with conceptualization, formal analysis, Methodology, and visualization. Varón-Ramírez, Gómez-Latorre, and Arroyo-Cruz contributed to the data curation and writing - original draft preparation. Arroyo-Cruz, Gómez-Tagle, Prado, Lobo-Lujan, Gutierrez, and Guevara contributed to Project administration and writing - review and editing. Prado and Guevara contributed to funding acquisition. .

Competing interests. The authors declare that they have no conflict of interest.

425 *Acknowledgements.* The authors want to thank to the National Meteorological Service (SMN by its initials in Spanish) and National Water Commission (CONAGUA by its initials in Spanish) for making public available the national climate data. Viviana Varón-Ramírez, Blanca Prado, and Mario Guevara acknowledges support from grant CF-2023-I-1846 of the National Council of Humanities, Sciences, and Technologies; abbreviated CONAHCYT. Mario Guevara acknowledges support from grant IGCP-765-UNESCO.



References

- 430 Adeyeri, O., Laux, P., Ishola, K., Zhou, W., Balogun, I., Adeyewa, Z., and Kunstmann, H.: Homogenising meteorological variables: Impact on trends and associated climate indices, *Journal of Hydrology*, 607, 127585, <https://doi.org/https://doi.org/10.1016/j.jhydrol.2022.127585>, 2022.
- Agustín Breña-Naranjo, J., Pedrozo-Acuña, A., Pozos-Estrada, O., Jiménez-López, S. A., and López-López, M. R.: The contribution of tropical cyclones to rainfall in Mexico, *Physics and Chemistry of the Earth, Parts A/B/C*, 83-84, 111–122, <https://doi.org/https://doi.org/10.1016/j.pce.2015.05.011>, emerging science and applications with microwave remote sensing data, 2015.
- 435 Alexandersson, H.: A homogeneity test applied to precipitation data, *Journal of Climatology*, 6, 661–675, <https://doi.org/https://doi.org/10.1002/joc.3370060607>, 1986.
- Alves, G. J., Mello, C. R., Guo, L., and Thebaldi, M. S.: Natural disaster in the mountainous region of Rio de Janeiro state, Brazil: Assessment of the daily rainfall erosivity as an early warning index, *International Soil and Water Conservation Research*, 10, 547–556, <https://doi.org/https://doi.org/10.1016/j.iswcr.2022.02.002>, 2022.
- 440 Beguería, S., Serrano-Notivol, R., and Tomas-Burguera, M.: Computation of rainfall erosivity from daily precipitation amounts, *Science of The Total Environment*, 637-638, 359–373, <https://doi.org/https://doi.org/10.1016/j.scitotenv.2018.04.400>, 2018.
- Benites, E. T., Becerra, J. C., Gil, J. U., Cedillo, L. T., and Torres, P. S. R.: Predicción de la erosión hídrica en la cuenca del Cañón del Sumidero, Chiapas, *Revista Mexicana de Ciencias Agrícolas*, 11, 1903–1915, <https://doi.org/10.29312/remexca.v11i8.2747>, epub 13 de diciembre de 2021, 2020.
- 445 Bessenbacher, V., Schumacher, D. L., Hirschi, M., Seneviratne, S. I., and Gudmundsson, L.: Gap-Filled Multivariate Observations of Global Land–Climate Interactions, *Journal of Geophysical Research: Atmospheres*, 128, e2023JD039099, <https://doi.org/https://doi.org/10.1029/2023JD039099>, e2023JD039099 2023JD039099, 2023.
- Bezak, N., Borrelli, P., and Panagos, P.: Exploring the possible role of satellite-based rainfall data in estimating inter- and intra-annual global rainfall erosivity, *Hydrology and Earth System Sciences*, 26, 1907 – 1924, <https://doi.org/10.5194/hess-26-1907-2022>, cited by: 26; All Open Access, Gold Open Access, Green Open Access, 2022.
- 450 Bolaños González, M. A., Paz Pellat, F., Cruz Gaistardo, C. O., Argumedo Espinoza, J. A., Romero Benítez, V. M., and de la Cruz Cabrera, J. C.: Mapa de erosión de los suelos de México y posibles implicaciones en el almacenamiento de carbono orgánico del suelo, *Terra Latinoamericana*, 34, 271–288, http://www.scielo.org.mx/scielo.php?script=sci_arttext&pid=S0187-57792016000300271&lng=es&tlng=es, recuperado en 03 de septiembre de 2024, 2016.
- 455 Borrelli, P., Robinson, D., Fleischer, L. R., Lugato, E., Ballabio, C., Alewell, C., Meusburger, M., Modugno, P., Schütt, M., Tenuta, K. E., and Panagos, P.: Land use and climate change impacts on global soil erosion by water (2015-2070), *Proceedings of the National Academy of Sciences*, 117, 21994–22001, <https://doi.org/10.1073/pnas.2001403117>, 2020.
- Cardoso, D. P., Silva, E. M., Avanzi, J. C., Muniz, J. A., Ferreira, D. F., Silva, M. L. N., Acuña-Guzman, S. F., and Curi, N.: RainfallErosivityFactor: An R package for rainfall erosivity (R-factor) determination, *CATENA*, 189, 104509, <https://doi.org/https://doi.org/10.1016/j.catena.2020.104509>, 2020.
- 460 Carrera, J. J., Levresse, G. P., and Hernández-Espriú, J. A.: Geostatistical Analysis of Yearly Precipitation at the National Level: Stratification and Anisotropy Considerations in Mexico, pre-print available at SSRN: <https://ssrn.com/abstract=4820011> or <http://dx.doi.org/10.2139/ssrn.4820011>, 2024.



- 465 Cespedes, J. M. N., Anguiano, J. H. H., Concepción, P. C. A., Martínez, J. L. M., Aguilera, G. C., and Padilla, F.: A comparison of missing value imputation methods applied to daily precipitation in a semi-arid and a humid region of Mexico, *Atmosfera*, 37, 33 – 52, <https://doi.org/10.20937/ATM.53095>, cited by: 3; All Open Access, Green Open Access, Hybrid Gold Open Access, 2023.
- Chen, Y., Xu, M., Wang, Z., Chen, W., and Lai, C.: Reexamination of the Xie model and spatiotemporal variability in rainfall erosivity in mainland China from 1960 to 2018, *CATENA*, 195, 104 837, <https://doi.org/https://doi.org/10.1016/j.catena.2020.104837>, 2020.
- 470 Commission for Environmental Cooperation: Ecological Regions of North America -Toward a Common Perspective, Commission for Environmental Cooperation, Montreal, Canada, ISBN 2-922305-20-1, 1997.
- Cuervo-Robayo, A. P., Téllez-Valdés, O., Gómez-Albores, M. A., Venegas-Barrera, C. S., Manjarrez, J., and Martínez-Meyer, E.: An update of high-resolution monthly climate surfaces for Mexico, *International Journal of Climatology*, 34, 2427 – 2437, <https://doi.org/10.1002/joc.3848>, cited by: 153, 2014.
- 475 Cuervo-Robayo, A. P., Ureta, C., Gómez-Albores, M. A., Meneses-Mosquera, A. K., Téllez-Valdés, O., and Martínez-Meyer, E.: One hundred years of climate change in Mexico, *PLOS ONE*, 15, 1–19, <https://doi.org/10.1371/journal.pone.0209808>, 2020.
- Das, S., Jain, M. K., Gupta, V., McGehee, R. P., Yin, S., de Mello, C. R., Azari, M., Borrelli, P., and Panagos, P.: GloRESatE: A dataset for global rainfall erosivity derived from multi-source data, *Scientific Data*, 11, 926, <https://doi.org/10.1038/s41597-024-03756-5>, 2024.
- de Anda Sánchez, J.: Precipitation in Mexico, pp. 1–14, Springer International Publishing, Cham, ISBN 978-3-030-40686-8, 480 https://doi.org/10.1007/978-3-030-40686-8_1, 2020.
- Duarte, L. V., Formiga, K. T. M., and Costa, V. A. F.: Comparison of Methods for Filling Daily and Monthly Rainfall Missing Data: Statistical Models or Imputation of Satellite Retrievals?, *Water*, 14, <https://doi.org/10.3390/w14193144>, 2022.
- Dunkerley, D. L.: Rainfall intensity bursts and the erosion of soils: an analysis highlighting the need for high temporal resolution rainfall data for research under current and future climates, *Earth Surface Dynamics*, 7, 345–360, <https://doi.org/10.5194/esurf-7-345-2019>, 2019.
- 485 Efthimiou, N.: Evaluating the performance of different empirical rainfall erosivity (R) factor formulas using sediment yield measurements, *CATENA*, 169, 195–208, <https://doi.org/https://doi.org/10.1016/j.catena.2018.05.037>, 2018.
- Feng, Z., Zhang, Z., Zuo, Y., Wan, X., Wang, L., Chen, H., Xiong, G., Liu, Y., Tang, Q., and Liang, T.: Analysis of long term water quality variations driven by multiple factors in a typical basin of Beijing-Tianjin-Hebei region combined with neural networks, *Journal of Cleaner Production*, 382, 135 367, <https://doi.org/https://doi.org/10.1016/j.jclepro.2022.135367>, 2023.
- 490 Fenta, A. A., Tsunekawa, A., Haregeweyn, N., Yasuda, H., Tsubo, M., Borrelli, P., Kawai, T., Sewale Belay, A., Ebabu, K., Liyew Berihun, M., Sultan, D., Asamin Setargie, T., Elnashar, A., and Panagos, P.: Improving satellite-based global rainfall erosivity estimates through merging with gauge data, *Journal of Hydrology*, 620, <https://doi.org/10.1016/j.jhydrol.2023.129555>, cited by: 15; All Open Access, Hybrid Gold Open Access, 2023.
- Fransiska, H., Agustina, D., Setyorini, D., Sumartajaya, I. M., and Kurnia, A.: Time Series Clustering Analysis Using Dynamic Time 495 Warping Technique of Daily Rainfall in Bengkulu Province, *IOP Conference Series: Earth and Environmental Science*, 1359, 012 026, <https://doi.org/10.1088/1755-1315/1359/1/012026>, 2024.
- Funk, C., Peterson, P., Landsfeld, M., Pedreros, D., Verdin, J., Shukla, S., Husak, G., Rowland, J., Harrison, L., Hoell, A., and Michaelsen, J.: The climate hazards infrared precipitation with stations—a new environmental record for monitoring extremes, *Scientific Data*, 2, 150 066, <https://doi.org/10.1038/sdata.2015.66>, 2015.
- 500 García-Cueto, O. R., Santillán-Soto, N., López-Velázquez, E., Reyes-López, J., Cruz-Sotelo, S., and Ojeda-Benítez, S.: Trends of climate change indices in some Mexican cities from 1980 to 2010, *Theoretical and Applied Climatology*, 137, 775–790, <https://doi.org/10.1007/s00704-018-2620-4>, 2019.



- González, O. N., Serrano, J. I. B., Vílchez, F. F., Núñez, R. M. M., and García-Sancho, A. G.: Riesgo de erosión hídrica y estimación de pérdida de suelo en paisajes geomorfológicos volcánicos en México, *Cultivos Tropicales*, 37, 45–55, http://scielo.sld.cu/scielo.php?script=sci_arttext&pid=S0258-59362016000200006&lng=es&tlng=es, recuperado en 02 de septiembre de 2024, 2016.
- 505 Guijarro, J. A.: Quality control and homogenization of climatological series, <https://doi.org/10.1201/b15625>, cited by: 5, 2014.
- Guijarro, J. A.: climatol: Climate Tools (Series Homogenization and Derived Products), <https://CRAN.R-project.org/package=climatol>, r package version 4.1.0, 2024.
- Gómez-Latorre, D. A., Araujo-Carrillo, G. A., and Leguizamón, Y. R.: Regionalización de patrones de lluvias para períodos multianuales secos y húmedos en el Altiplano Cundiboyacense de Colombia, *Revista de Climatología*, 22, 162–177, <https://rclimatol.eu/2022/12/31/regionalizacion-de-patrones-de-lluvias-para-periodos-multianuales-secos-y-humedos-en-el-altiplano-cundiboyacense-de-colombia/>, 2022.
- 510 Hartigan, J. A.: Clustering algorithms, John Wiley & Sons, Inc., 1975.
- Hatfield, J. L., Sauer, T. J., and Cruse, R. M.: Chapter One - Soil: The Forgotten Piece of the Water, Food, Energy Nexus, *Advances in Agronomy*, 143, 1–46, <https://doi.org/https://doi.org/10.1016/bs.agron.2017.02.001>, 2017.
- 515 Hirca, T. and Türkkan, G. E.: Assessment of Different Methods for Estimation of Missing Rainfall Data, *Water Resources Management*, <https://doi.org/10.1007/s11269-024-03936-3>, published online on 2024/07/31, 2024.
- INEGI-CONABIO-INE: Ecorregiones Terrestres de México, Tech. rep., Instituto Nacional de Estadística, Geografía e Informática (INEGI) and Comisión Nacional para el Conocimiento y Uso de la Biodiversidad (CONABIO) and Instituto Nacional de Ecología (INE), México, escala 1:1000000, 2008.
- 520 Ke, Q. and Zhang, K.: Patterns of runoff and erosion on bare slopes in different climate zones, *CATENA*, 198, 105–109, <https://doi.org/https://doi.org/10.1016/j.catena.2020.105069>, 2021.
- Li, J., Sun, R., and Chen, L.: Assessing the accuracy of large-scale rainfall erosivity estimation based on climate zones and rainfall patterns, *CATENA*, 217, 106–118, <https://doi.org/https://doi.org/10.1016/j.catena.2022.106508>, 2022.
- 525 Lupi, A., Luppichini, M., Barsanti, M., Bini, M., and Giannecchini, R.: Machine learning models to complete rainfall time series databases affected by missing or anomalous data, *Earth Science Informatics*, 16, 3717–3728, <https://doi.org/10.1007/s12145-023-01122-4>, 2023.
- Mateos, E., Santana, J.-S., Montero-Martínez, M. J., Deeb, A., and Grunwaldt, A.: Possible climate change evidence in ten Mexican watersheds, *Physics and Chemistry of the Earth, Parts A/B/C*, 91, 10–19, <https://doi.org/https://doi.org/10.1016/j.pce.2015.08.009>, appropriate Technology and Climate Change Adaptation for Water Resources Management, 2016.
- 530 McCuen, R. H.: Hydrologic Analysis and Design, Pearson, 4th edition edn., ISBN 978-0134313122, 2016.
- McKinnon, K. A.: Discussion on “A combined estimate of global temperature”, *Environmetrics*, 33, e2721, <https://doi.org/https://doi.org/10.1002/env.2721>, 2022.
- Meng, X., Zhu, Y., Yin, M., and Liu, D.: The impact of land use and rainfall patterns on the soil loss of the hillslope, *Scientific Reports*, 11, 16341, <https://doi.org/10.1038/s41598-021-95819-5>, 2021.
- 535 Musgrave, G.: The quantitative evaluation of factors in water erosion—a first approximation., *J. Soil Water Conserv.*, 2, 133–138, 1947.
- Nearing, M. A.: Soil Erosion and Conservation, p. Chapter page numbers if available, Wiley, 2nd edn., <https://digitalcommons.unl.edu/usdaarsfacpub/1290/>, 2013.
- Nearing, M. A., qing Yin, S., Borrelli, P., and Polyakov, V. O.: Rainfall erosivity: An historical review, *CATENA*, 157, 357–362, <https://doi.org/https://doi.org/10.1016/j.catena.2017.06.004>, 2017.



- 540 Panagos, P., Borrelli, P., Meusburger, K., Yu, B., Klik, A., Jae Lim, K., Yang, J. E., Ni, J., Miao, C., Chattopadhyay, N., Sadeghi, S. H., Hazbavi, Z., Zabihi, M., Larionov, G. A., Krasnov, S. F., Gorobets, A. V., Levi, Y., Erpul, G., Birkel, C., Hoyos, N., Naipal, V., Oliveira, P. T. S., Bonilla, C. A., Meddi, M., Nel, W., Al Dashti, H., Boni, M., Diodato, N., Van Oost, K., Nearing, M., and Ballabio, C.: Global rainfall erosivity assessment based on high-temporal resolution rainfall records, *Scientific Reports*, 7, 4175, <https://doi.org/10.1038/s41598-017-04282-8>, 2017.
- 545 Panagos, P., Hengl, T., Wheeler, I., Marcinkowski, P., Rukeza, M. B., Yu, B., Yang, J. E., Miao, C., Chattopadhyay, N., Sadeghi, S. H., Levi, Y., Erpul, G., Birkel, C., Hoyos, N., Oliveira, P. T. S., Bonilla, C. A., Nel, W., Al Dashti, H., Bezak, N., Van Oost, K., Petan, S., Fenta, A. A., Haregeweyn, N., Pérez-Bidegain, M., Liakos, L., Ballabio, C., and Borrelli, P.: Global rainfall erosivity database (GloREDA) and monthly R-factor data at 1 km spatial resolution, *Data in Brief*, 50, 109 482, <https://doi.org/https://doi.org/10.1016/j.dib.2023.109482>, 2023.
- 550 Paulhus, J. L. H. and Kohler, M. A.: Interpolation of missing precipitation records, *Monthly Weather Review*, 80, 129–133, [https://doi.org/10.1175/1520-0493\(1952\)080<0129:IOMPR>2.0.CO;2](https://doi.org/10.1175/1520-0493(1952)080<0129:IOMPR>2.0.CO;2), 1952.
- Pennock, D.: Soil erosion: the greatest challenge for sustainable soil management, FAO, Rome, Italy, ISBN 978-92-5-131426-5, <https://openknowledge.fao.org/items/6c070e1e-6533-4b7e-ba5f-a2f21a0e59ff>, 2019.
- Pineda-Martínez, L. F. and Carbajal, N.: Climatic analysis linked to land vegetation cover of Mexico by applying multivariate statistical and clustering analysis, *Atmósfera*, 30, 233–242, <https://doi.org/10.20937/atm.2017.30.03.04>, 2017.
- 555 Porrúa, F. E., Hidalgo, J. Z., Arroyo, A. M., Raga, G., and García, C. G.: Estado y perspectivas del Cambio Climático en México: un punto de partida, Tech. rep., Universidad Nacional Autónoma de México, Mexico, ISBN 978-607-30-8172-6, <https://cambioclimatico.unam.mx/estado-y-perspectivas-del-cambio-climatico-en-mexico/>, 2020.
- R Core Team: R: A Language and Environment for Statistical Computing, R Foundation for Statistical Computing, Vienna, Austria, <https://www.R-project.org/>, 2022.
- 560 Renard, K. G. and Freimund, J. R.: Using monthly precipitation data to estimate the R-factor in the revised USLE, *Journal of Hydrology*, 157, 287–306, <https://api.semanticscholar.org/CorpusID:5030732>, 1994.
- Richardson, C. W., Foster, G. R., and Wright, D.: Estimation of Erosion Index from Daily Rainfall Amount, *Transactions of the ASABE*, 26, 153–0156, <https://api.semanticscholar.org/CorpusID:108883838>, 1983.
- 565 Rohlf, F. J.: Methods of comparing classifications, *Annual Review of Ecology and Systematics*, 5, 101–113, 1974.
- Shin, J.-Y., Kim, T., Heo, J.-H., and Lee, J.-H.: Spatial and temporal variations in rainfall erosivity and erosivity density in South Korea, *CATENA*, 176, 125–144, <https://doi.org/https://doi.org/10.1016/j.catena.2019.01.005>, 2019.
- Todeschini, R., Ballabio, D., Termopoli, V., and Consonni, V.: Extended multivariate comparison of 68 cluster validity indices. A review, *Chemometrics and Intelligent Laboratory Systems*, p. 105117, <https://doi.org/https://doi.org/10.1016/j.chemolab.2024.105117>, 2024.
- 570 Torres, H. G. C.: Caracterización de la erosividad de la lluvia en México utilizando métodos multivariados, Master's thesis, Colegio de Posgraduados, Montecillo, Mexico, centro de Edafología, 1991.
- Tu, A., Xie, S., Li, Y., Liu, Z., and Shen, F.: Effect of fixed time interval of rainfall data on calculation of rainfall erosivity in the humid area of south China, *CATENA*, 220, 106 714, <https://doi.org/https://doi.org/10.1016/j.catena.2022.106714>, 2023.
- Vantas, K., Sidiropoulos, E., and Evangelides, C.: Rainfall Erosivity and Its Estimation: Conventional and Machine Learning Methods, in: *Soil Erosion*, edited by Hrissanthou, V. and Kaffas, K., chap. 2, IntechOpen, Rijeka, <https://doi.org/10.5772/intechopen.85937>, 2019.



- Varón-Ramírez, V., Gómez-Latorre, D., Arroyo-Cruz, C., Guevara Santamaría, M., and Prado Pano, B.: Daily rainfall series and rainfall erosivity in Mexico for three climatic normals (1968-1997, 1978-2007, and 1988-2017) ver 1, <https://doi.org/10.6073/pasta/7479676e406aeb40127da7b096b28eb2>, accessed 2024-09-18, 2024.
- Varón-Ramírez, V. M.: VimiVaron/Rainfall-Erosivity-Mexico: Rainfall- Erosivity-Mexico, <https://doi.org/10.5281/zenodo.13830947>, 2024.
- 580 Varón-Ramírez, V. M. and Guevara, M.: Advances in the study of soil erosion by water in Mexico published in Spanish, *European Journal of Soil Science*, 75, e13 458, <https://doi.org/https://doi.org/10.1111/ejss.13458>, 2024.
- Vaughan, C., Buja, L., Kruczkiewicz, A., and Goddard, L.: Identifying research priorities to advance climate services, *Climate Services*, 4, 65–74, <https://doi.org/https://doi.org/10.1016/j.cliser.2016.11.004>, 2016.
- Wischmeier, W. H. and Smith, D. D.: Predicting rainfall erosion losses : a guide to conservation planning, <https://api.semanticscholar.org/CorpusID:129088976>, 1978.
- 585
- WMO: Guidelines on Homogenization. WMO-No. 1245, <https://library.wmo.int/idurl/4/57130>, 2020.
- WMO: Guide to Climatological Practices. WMO-No. 100, <https://library.wmo.int/idurl/4/60113>, 2023.
- World Meteorological Organization: WMO Guidelines on the Calculation of Climate Normals, <https://library.wmo.int/es/records/item/55797-wmo-guidelines-on-the-calculation-of-climate-normals>, 2017.
- 590 World Meteorological Organization: Guidelines on Homogenization, https://dgm-meteo.github.io/wmo-clino/Docs/WMO2020_1245_en_Guidelines%20on%20Homogenization.pdf, wMO-No. 1245, 2020.
- Xie, Y., qing Yin, S., yuan Liu, B., Nearing, M. A., and Zhao, Y.: Models for estimating daily rainfall erosivity in China, *Journal of Hydrology*, 535, 547–558, <https://doi.org/https://doi.org/10.1016/j.jhydrol.2016.02.020>, 2016.
- Yan, Z., Li, Z., and Xia, J.: Homogenization of climate series: The basis for assessing climate changes, *Science China Earth Sciences*, 57, 2891–2900, <https://doi.org/10.1007/s11430-014-4945-x>, 2014.
- 595
- Yin, S., Xie, Y., Liu, B., and Nearing, M. A.: Rainfall erosivity estimation based on rainfall data collected over a range of temporal resolutions, *Hydrology and Earth System Sciences*, 19, 4113–4126, <https://doi.org/10.5194/hess-19-4113-2015>, 2015.
- Yozgatligil, C., Aslan, S., Iyigun, C., and Batmaz, I.: Comparison of missing value imputation methods in time series: the case of Turkish meteorological data, *Theoretical and Applied Climatology*, 112, 143–167, <https://doi.org/10.1007/s00704-012-0723-x>, 2013.
- 600 Yu, B. and Rosewell, C. J.: Rainfall erosivity estimation using daily rainfall amounts for South Australia, *Soil Research*, 34, 721–733, <https://api.semanticscholar.org/CorpusID:128543482>, 1996.
- Zhao, B., Zhang, L., Xia, Z., Xu, W., Xia, L., Liang, Y., and Xia, D.: Effects of Rainfall Intensity and Vegetation Cover on Erosion Characteristics of a Soil Containing Rock Fragments Slope, *Advances in Civil Engineering*, 2019, 7043 428, <https://doi.org/https://doi.org/10.1155/2019/7043428>, 2019.